

Modeling short-range-ordering in liquids: the Mg-Al-Sn system

Youn-Bae Kang and Arthur D. Pelton

Centre de Recherche en Calcul Thermochimique (CRCT), Département de Génie Chimique, École Polytechnique, P.O. Box 6079, Station "Downtown", Montréal, CANADA, H3C 3A7, Phone: (1) 514 340 4711 ext. 4531 - Fax: (1) 514 340 5840

October 3, 2009

Abstract:

A liquid solution of components A and B may often exhibit a tendency towards short-range-ordering (SRO). This may be modeled by the Modified Quasichemical Model (MQM) which attributes the SRO to the preferential formation of nearest-neighbor A-B pairs or, alternatively, by an associate model which attributes the ordering to the formation of A_nB_m associates or molecules. Although both models can often provide similar and equally good fits to experimental thermodynamic and phase equilibrium data in a binary system, the MQM provides significantly better predictions of the thermodynamic properties of ordered ternary liquid phases A-B-C solely from the optimized model parameters of the A-B, B-C and C-A binary sub-systems. This is illustrated through coupled thermodynamic/phase diagram optimization of the Mg-Al-Sn system. Similar examples for the Mg-Al-Sc and $AlCl_3$ -NaCl-KCl systems are also presented.

Key words:

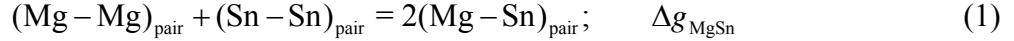
Modified quasichemical model, solution models, liquids, Mg-Al-Sn system, Mg-Al-Sc system

1. Introduction

A thermodynamic model for a solution should not only reproduce the data for binary systems, but should also predict as closely as possible the properties of ternary and higher-order solutions from the optimized binary parameters.

As is well-known, short-range-ordering (SRO) in binary liquid solutions is evidenced by enthalpy of mixing curves which exhibit a relatively sharp negative peak, as opposed to the more parabolic shape characteristic of solutions with no appreciable SRO. An example, for Mg-Sn liquid solutions, is shown in Fig. 1; the composition of maximum SRO occurs near the mole fraction $X_{Sn} = 1/3$. The corresponding entropy of mixing curve, typical of SRO, is shown in Fig. 2. The corresponding partial excess Gibbs energy curves are shown in Fig. 3; these typically exhibit inflection points near the composition of maximum SRO. Such solutions have been modeled by the Modified Quasichemical Model (MQM) or by "associate" models.

In the MQM, which has been used extensively in the authors' research group, the SRO is modeled as a preference for the formation of (Mg-Sn) nearest-neighbor pairs. That is, the Mg and Sn atoms are distributed on a quasilattice, and the following exchange reaction among nearest-neighbor pairs is at equilibrium:



The principal model parameter is the Gibbs energy change, Δg_{MgSn} of this reaction. If this parameter is negative, then reaction (1) is displaced to the right and (Mg-Sn) pairs are favored. In order to set the composition of maximum SRO at the observed composition of $X_{\text{Sn}} = 1/3$, the ratio of the coordination numbers of Sn and Mg is set to $Z_{\text{Sn}}/Z_{\text{Mg}} = 2$. (In the limit of a very large negative Δg_{MgSn} , the solution is fully ordered at $X_{\text{Sn}} = 1/3$, with Mg atoms surrounded only by Sn atoms and Sn atoms only by Mg atoms.)

In the associate model, the SRO is modeled as due to the formation of Mg_2Sn “associates” or molecules. That is, Mg atoms, Sn atoms and Mg_2Sn molecules are randomly distributed over the sites of a single quasilattice. The principal model parameter is the Gibbs energy change for the formation of Mg_2Sn associates from unassociated Mg and Sn atoms:



If this parameter is negative, then reaction (2) is displaced to the right. (In the limit of a very large negative parameter, the solution would be fully ordered at $X_{\text{Sn}} = 1/3$ where it would consist of only Mg_2Sn associates, each occupying one lattice site.)

Although, in our opinion, the MQM is the more physically realistic, in many binary systems the two models can provide very similar and equally good fits to the experimental thermodynamic and phase diagram data with approximately the same number of model parameters. That is, the two models are mathematically very similar in binary solutions.

However, this is no longer true in ternary and higher-order solutions. Consider for example the Mg-Al-Sn ternary phase diagram shown in Fig. 4. In this system, the Mg-Sn binary liquid solution exhibits appreciable SRO as discussed above, while the Mg-Al and Al-Sn binary liquid solutions exhibit relatively little. Along the join from the Al-corner to the Mg-Sn side of the composition triangle, positive deviations from ideal mixing of the liquid phase are evident as witnessed by the widely-spaced liquidus isotherms and by the appearance of a liquid-liquid immiscibility gap. Such behavior is typical of ternary systems in which one binary liquid exhibits large negative deviations from ideality relative to the other two binary liquids.

The MQM predicts this behaviour. Since (Mg - Sn) nearest-neighbor pairs are energetically favored, the model predicts a tendency for the liquid phase to separate into clusters rich in (Mg-Sn) pairs and clusters rich in Al. The associate model, on the other hand, fails entirely to predict this behavior. Along the Al- Mg_2Sn join, the associate model predicts an approximately ideal mixture of Al atoms and Mg_2Sn associates, and the observed positive deviations in the ternary system can only be reproduced by introducing additional adjustable ternary model parameters optimized to fit ternary experimental data.

The present article begins with a brief summary of the model equations. Following this, an optimization of the Mg-Sn binary system is presented with the MQM used for the liquid phase. A new optimization of the Al-Sn binary system is also presented. Thereafter it is shown that all available experimental phase equilibrium and thermodynamic data in the Mg-Al-Sn ternary system are predicted by the MQM solely from the binary model parameters with no additional ternary terms, and comparison is made with predictions using the associate model.

A second example is then given for the similar Mg-Al-Sc system, where again it is shown that the ternary phase diagram is predicted with good precision solely from the optimized binary MQM parameters for the liquid phase. Finally, an example for a molten salt system is presented.

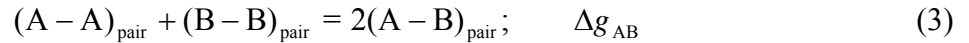
All calculations in the present study were performed using the FactSage software and databases [1,2].

2. Model equations

2.1 The Modified Quasichemical Model

The detailed development of the MQM has been given previously for binary [3] and for multicomponent [4] solutions. Only an outline will be presented here.

The quasichemical model, in the pair approximation first proposed by Fowler and Guggenheim [5] and later extended by Blander, Pelton, Chartrand and co-workers [3, 4, 6], models SRO as the preferential formation of first-nearest-neighbor (A–B) pairs. In the simplest case, the A and B atoms or molecules are assumed to be distributed on a quasilattice, and the following exchange reaction among nearest-neighbor pairs is at equilibrium:



where Δg_{AB} is the Gibbs energy change of this quasichemical reaction for the formation of two moles of (A–B) pairs. Let Z_A and Z_B be the nearest-neighbor coordination numbers of A and B. Hence, each A or B atom forms Z_A and Z_B pairs respectively, and so for one mole of solution:

$$Z_A n_A = 2n_{AA} + n_{AB} \quad (4)$$

$$Z_B n_B = 2n_{BB} + n_{AB} \quad (5)$$

where n_A and n_B are the numbers of moles of A and B and n_{AA} , n_{BB} and n_{AB} are the numbers of moles of pairs. Pair fractions X_{ij} are defined as:

$$X_{ij} = n_{ij} / (n_{AA} + n_{BB} + n_{AB}) \quad (6)$$

The Gibbs energy of mixing is assumed to be given by:

$$\Delta G = (n_{AB}/2)\Delta g_{AB} - T\Delta S^{\text{config}} \quad (7)$$

The configurational entropy ΔS^{config} is given by randomly distributing the first-nearest-neighbor pairs over “pair positions”. In three dimensions the exact mathematical expression is unknown; an approximate expression is obtained as follows. If the pairs are distributed with no regard for overlap, then a molar entropy of $-R[(Z_A X_A + Z_B X_B)/2](X_{AA} \ln X_{AA} + X_{BB} \ln X_{BB} + X_{AB} \ln X_{AB})$ results (where X_A and X_B are the mole fractions and where the factor $[(Z_A X_A + Z_B X_B)/2]$ is the number of moles of bonds per mole of solution.) This expression clearly overestimates the number of possible configurations because, for example, an (A–A) and a (B–B) pair cannot both contain the same central atom. A correction is applied by considering that when $\Delta g_{AB} = 0$, the solution should be a random mixture with an ideal configurational entropy and with $X_{AA} = Y_A^2$, $X_{BB} = Y_B^2$ and $X_{AB} = 2Y_A Y_B$, where:

$$Y_A = Z_A X_A / (Z_A X_A + Z_B X_B) = (1 - Y_B) \quad (8)$$

As shown previously [3], the following expression results:

$$\begin{aligned} \Delta S^{\text{config}} = & -R(n_A \ln X_A + n_B \ln X_B) \\ & -R[n_{AA} \ln(\frac{X_{AA}}{Y_A^2}) + n_{BB} \ln(\frac{X_{BB}}{Y_B^2}) + n_{AB} \ln(\frac{X_{AB}}{2Y_A Y_B})] \end{aligned} \quad (9)$$

Minimizing the Gibbs energy subject to the constraints of Eqs. (4,5) yields the following “quasichemical equilibrium constant” for reaction (3):

$$\frac{X_{AB}^2}{X_{AA} X_{BB}} = 4 \exp(-\frac{\Delta g_{AB}}{RT}) \quad (10)$$

At a given composition and for a given value of Δg_{AB} , Eqs. (4,5,10) can be solved to give X_{ij} which can then be substituted back into Eqs. (7,9). When $\Delta g_{AB} = 0$, the solution is a random ideal solution. As Δg_{AB} becomes progressively more negative, reaction (3) is displaced progressively to the right and the degree of SRO increases.

For purposes of optimization, Δg_{AB} is expanded [3] as a polynomial in the bond fractions:

$$\Delta g_{AB} = \Delta g_{AB}^{\circ} + \sum_{i \geq 1} g_{AB}^{i0} X_{AA}^i + \sum_{j \geq 1} g_{AB}^{0j} X_{BB}^j \quad (11)$$

where Δg_{AB}° , g_{AB}^{i0} and g_{AB}^{0j} are the adjustable model parameters. Alternatively [3], Δg_{AB} may be expanded as a polynomial in the component fractions Y_A and Y_B .

Eq. (9) for the entropy can be shown [6, 7] to be exact only for a one-dimensional lattice ($Z = 2$). In three dimensions the equation is only approximate as no exact solution of the ‘‘three-dimensional Ising model’’ is known. As discussed previously [3, 7], the error introduced by this approximation can be offset through the choice of somewhat non-physical values of Z . From our experience in applying the MQM to many liquid metallic solutions, we have found that a value of approximately $Z = 6$ generally yields the best results, although the calculations are not highly sensitive to this parameter. Of course, if the composition of maximum SRO is observed at a composition other than $X_A = X_B = 1/2$, then Z_A and Z_B cannot both be equal. For example, as discussed in the previous section, the composition of maximum SRO in the Mg-Sn system occurs at $X_{Sn} = 1/3$, such that the ratio Z_{Sn}/Z_{Mg} should be set equal to 2.0. For greater flexibility, we permit Z_A and Z_B to vary with composition as follows [3]:

$$\frac{1}{Z_A} = \frac{1}{Z_{AA}^A} \left(\frac{2n_{AA}}{2n_{AA} + n_{AB}} \right) + \frac{1}{Z_{AB}^A} \left(\frac{n_{AB}}{2n_{AA} + n_{AB}} \right) \quad (12)$$

$$\frac{1}{Z_B} = \frac{1}{Z_{BB}^B} \left(\frac{2n_{BB}}{2n_{BB} + n_{AB}} \right) + \frac{1}{Z_{BA}^B} \left(\frac{n_{AB}}{2n_{BB} + n_{AB}} \right) \quad (13)$$

where Z_{AA}^A and Z_{AB}^A are the values of Z_A respectively when all nearest neighbors of an A are A's and when all nearest neighbors of an A are B's, and where Z_{BB}^B and Z_{BA}^B are defined similarly.

In order to set the composition of maximum SRO at $X_{Sn} = 1/3$, it is only required that $Z_{SnMg}^{Sn}/Z_{MgSn}^{Mg} = 2.0$. Hence, we set $Z_{MgMg}^{Mg} = Z_{SnSn}^{Sn} = 6.0$ for the pure elements, while setting $Z_{MgSn}^{Mg} = 4.0$ and $Z_{SnMg}^{Sn} = 8.0$ (such that their average is 6.0). The choice of values for Z_{ij} has been discussed in detail previously [7].

For a ternary liquid solution A-B-C, the Gibbs energy of mixing is given by [4]:

$$\Delta G = (n_{AB}/2)\Delta g_{AB} + (n_{BC}/2)\Delta g_{BC} + (n_{CA}/2)\Delta g_{CA} - T\Delta S^{\text{config}} + (\text{ternary terms}) \quad (14)$$

where Δg_{AB} , Δg_{BC} and Δg_{CA} are the binary parameters obtained from optimization of the three binary sub-systems, and where the expression for ΔS^{config} is given by randomly distributing all $(i-j)$ pairs ($i, j = A, B, C$) over the pair positions, resulting in an entropy expression similar to Eq. (9). Detailed equations for calculating the values of the parameters Δg_{ij} at a composition point in the ternary system from their optimized values in the binary sub-systems have been given previously [4]. The parameters of the additional (ternary terms) in

Eq. (14) are obtained by optimization using ternary experimental data. Ideally, these terms should be zero or small.

2.2 Associate Model

Consider as example an associate model for the Mg-Al-Sn liquid solution. Mg atoms, Al atoms, Sn atoms and Mg₂Sn associates are randomly distributed on a quasilattice: (Mg, Sn, Al, Mg₂Sn). That is, the ternary solution is formally treated, using the usual Compound Energy Formalism [8], as a single-lattice 4-component solution with end-members Mg, Sn, Al and Mg₂Sn, where the Gibbs energy of formation from the elements of the pure end-member Mg₂Sn is a composition-independent model parameter obtained during optimization of the Mg-Sn binary system. Binary interaction terms ${}^kL_{ij}$ ($i, j = \text{Mg, Sn, Al, Mg}_2\text{Sn}$) between the species are included and are obtained during optimization of binary systems except for the parameters ${}^kL_{\text{Al, Mg}_2\text{Sn}}$ which are ternary parameters which cannot be obtained from the binary data and which must either be set to zero or obtained by optimization using ternary experimental data.

3. The Mg-Sn binary system

An optimization of this binary system, using the MQM for the liquid phase, has been presented by Jung *et al.* [9]. All available experimental data were reviewed by these authors. Experimental data for the enthalpy of liquid mixing, the excess Gibbs energy of the liquid phase, and the phase diagram are shown in Figs. 1, 3 and 5.

In the present re-optimization the properties of the pure elements are taken from Dinsdale [10]. We have retained the values of H_{298}° and C_p used by Jung *et al.* [9] for the line compound Mg₂Sn, but have taken the entropy S_{298}° from Jelinek *et al.* [11] who derived the value from their low-temperature C_p measurements. The (Mg)_{hcp} solution was modeled by a simple substitutional model, with the lattice stability of pure hcp Sn taken from Dinsdale [10]. The solubility of Mg in solid Sn was assumed negligible. The liquid phase parameters were re-optimized. All optimized parameters are listed in Table 1. As can be seen in Figs. 1, 3, 5, the experimental data are well reproduced. The calorimetrically determined enthalpy of fusion of Mg₂Sn as measured by Sommer *et al.* [12] (19.6 kJ/g-atom) is also well reproduced (calculated value = 19.4 kJ/g-atom.) The calculated entropy of the liquid solution is shown in Fig. 2.

This system was optimized, using the associate model for the liquid phase, by Fries and Lukas [13] and the model parameters for the liquid are found in Ref. [14]. The optimized thermodynamic properties and phase diagram are shown in Figs. 1, 2, 3 and 5. It can be seen that the MQM and the associate model yield very similar optimizations for the binary system.

4. The Al-Sn binary system

The phase diagram and enthalpy of liquid mixing are shown in Figs. 6 and 7. The solubility of Sn in solid (Al)_{fcc} was assumed negligible. The solubility of Al in solid (Sn)_{bct} was treated as a simple ideal substitutional solution [15] using the lattice stability of pure bct Al given by Dinsdale [10]. The liquid solution was modeled with the MQM. All model parameters are

shown in Table 1. As can be seen in Figs. 6 and 7, the experimental data are well reproduced. The liquid exhibits small positive deviations from ideal mixing. As a result, the parameter Δg_{AlSn} is slightly positive and the model predicts a small degree of clustering of Sn and Al. That is, reaction (3) is displaced slightly to the left.

5. The Mg-Al binary system

The Mg-Al binary phase diagram, as optimized by Chartrand [16] is shown in Fig. 8. For the liquid phase, the MQM was used. Optimized parameters for the liquid are given in reference [17]. (The parameters for the $(\text{Al})_{\text{fcc}}$ and $(\text{Mg})_{\text{hcp}}$ phases of the Mg-Al binary system given in reference [17] were in error. The correct parameters for these phases from Chartrand [16] are reproduced in Table 1). The parameter Δg_{MgAl} for the liquid is small and negative, indicating a small degree of SRO. The terminal solid solutions were treated as simple substitutional solutions. The β , ε , and γ phases were modeled as described by Chartrand [16].

6. The Mg-Al-Sn ternary system

Various phase diagram sections of the ternary Mg-Al-Sn system are shown in Figs. 9 to 11. The data of different authors can be seen to be in good agreement. Experimental enthalpies of liquid mixing [18] are shown in Figs. 12 and 13.

The phase diagram was calculated with the liquid properties predicted by the MQM with no ternary parameters. (The “symmetric approximation” as described in reference [4] was used.) All solid phases were assumed to have only unary or binary phase fields except for the $(\text{Mg})_{\text{hcp}}$ solution which was modeled as a simple substitutional solution using only the binary parameters in Table 1; the interaction parameters ${}^k L_{\text{AlSn}}$ were assumed to be negligible. The predicted phase diagram sections and enthalpies of liquid mixing are compared to the experimental data in Figs. 9-13. The agreement is very good. The calculated projection of the liquidus surface is shown in Fig. 4.

The phase diagram was calculated by Doernberg *et al.* [19] who used the associate model of Fries and Lukas [13] for the liquid Mg-Sn solution, while modeling the Al-Sn [15] and Mg-Al [20] liquid solutions as simple substitutional solutions with ideal configurational entropies. Calculated phase diagram sections and enthalpies of liquid mixing are shown in Figs. 9, 10, 12(a) and 13 for the cases where (1) no ternary parameters were used, and (2) where one ternary parameter $L_{\text{Al,Mg}_2\text{Sn}}$, optimized by Doernberg *et al.* [19] to fit the ternary data, was employed. As can be seen in these figures, the associate model with no ternary terms fails to predict the positive deviations from ideal mixing in the ternary liquid, as was discussed in Section 1. With the inclusion of the positive ternary parameter, the phase diagram is reproduced reasonably well in the central composition regions (Fig. 9). However, as can be seen in Fig. 10, even with a ternary parameter the agreement with the experimental data in other composition regions is not as good as that obtained with the MQM with no ternary parameters.

7. The Mg-Al-Sc ternary system

The projection of the liquidus surface of the Mg-Al-Sc system is shown in Fig. 14 and various sections of the phase diagram are shown in Figs. 15-17.

The Mg-Al [16], Al-Sc [21], and Mg-Sc [21] binary systems have been optimized previously using the MQM for the liquid solutions. The Al-Sc liquid exhibits a high degree of SRO with the composition of maximum ordering near the composition AlSc. The Mg-Al and Mg-Sc liquid solutions exhibit only relatively small degrees of SRO.

The ternary phase diagram was calculated using only the binary MQM model parameters [16, 21] for the liquid. (The symmetric approximation as described in reference [4] was used.) The terminal solid solutions: $(\text{Mg})_{\text{hcp}}$, $(\text{Al})_{\text{fcc}}$, $(\text{Sc})_{\text{hcp}}$ and $(\text{Sc})_{\text{bcc}}$ were modeled as substitutional solutions using only the binary model parameters [16, 21]. (The Mg-rich and Sc-rich hcp solutions were modeled as a single phase with an immiscibility gap.) The solution of Mg_3Sc in Al_3Sc was modeled as a simple substitutional solution $(\text{Al}, \text{Mg})_3\text{Sc}$ with the Gibbs energy of the Mg_3Sc end-member ($G_{\text{Mg}_3\text{Sc}}$) and an interaction parameter ($L_{\text{Al},\text{Mg},\text{Sc}}$) chosen (see Table 1) so as to reproduce the measured solubility at 350°C as shown in Fig. 15. The solution of MgSc in AlSc was modeled with a two-sublattice Compound Energy Formalism $(\text{Mg}, \text{Al})[\text{Sc}, \text{Mg}]$ so as to reproduce the measured solubility at 350°C as shown in Fig. 15. The optimized parameters are shown in Table 1. The solubility of Mg_2Sc in Al_2Sc is negligible (~ 1 at.% Mg) [22]. Al_2Sc was thus treated as a stoichiometric (line) compound.

Calculated phase diagram sections are compared with the experimental data in Figs. 15 to 18. The agreement is very good. The calculated liquidus projection is shown in Fig. 14. The observed positive deviations along joins between the Mg-corner and the Al-Sc edge of the ternary composition triangle are predicted by the model, as discussed in Section 1. This is most clearly seen in Figs. 14 and 16.

The three binary sub-systems were re-optimized using an associate model for the binary Al-Sc liquid solution assuming AlSc associates. The Mg-Al and Mg-Sc binary liquids were modeled using a simple substitutional model with ideal configurational entropies of mixing with available model parameters [20, 23]. The ternary Mg-Al-Sc phase diagram was then calculated using only the binary model parameters. As is evident in Fig. 16, the positive deviations in the ternary liquid solution are not predicted by the associate model.

8. The AlCl_3 -NaCl-KCl ternary system

A final example for a ternary molten salt system is shown in Figs. 19 and 20. An optimization of this system was reported previously [54]. All parameters and details can be found in this reference. The MQM was used for the liquid phase. Strong SRO occurs around the composition KAlCl_4 in the $\text{KCl}-\text{AlCl}_3$ binary liquid. Similar SRO occurs in the $\text{NaCl}-\text{AlCl}_3$ binary liquid, but to a lesser degree. Consequently, positive deviations are observed along the $\text{NaCl}-\text{KAlCl}_4$ section as can be seen in Figs. 19 and 20. The liquidus along the join, calculated with no ternary parameters, compares favorably with the experimental data as can be seen in Fig. 20.

9. Conclusions

In Mg-Sn liquid alloys there is a relatively strong tendency towards SRO about the Mg_2Sn composition. This SRO has been modeled by the MQM which attributes the SRO to the preferential formation of nearest-neighbor Mg-Sn pairs. Similar optimizations of the Al-Sn and Mg-Al systems have also been performed using the MQM for the liquid phases. These binary liquids show a much lower tendency towards SRO. When the thermodynamic properties of the ternary liquid Mg-Al-Sn solutions are subsequently estimated using the MQM, excellent agreement with measured ternary phase diagram and thermodynamic data is obtained with no additional ternary parameters being required. In particular, the observed tendency to positive deviations from ideal mixing (tendency to immiscibility) along the Mg_2Sn -Al join are correctly predicted by the MQM as being due to the formation of clusters rich in Mg-Sn pairs and clusters rich in Al. If the SRO in the Mg-Sn liquid alloys is modeled using an associate model which attributes the SRO to the formation of Mg_2Sn associates or molecules, then equally good fits to the experimental data in the binary system can be obtained. However, the associate model does not correctly predict the properties of the Mg-Al-Sn liquid. In particular, it fails entirely to predict the observed positive deviations along the Mg_2Sn -Al join. Along this join the associate model predicts an approximately ideal mixture of Al atoms and Mg_2Sn associates, and the observed positive deviations can only be reproduced by introducing additional adjustable ternary model parameters optimized to fit the ternary experimental data.

Similar examples have also been presented for the Mg-Al-Sc and AlCl_3 -NaCl-KCl systems.

Acknowledgements

This research was supported by funding from the Natural Sciences and Engineering Research Council of Canada (NSERC) Magnesium Strategic Research Network. More information on the Network can be found at www.MagNET.ubc.ca.

References

- [1] C.W. Bale, P. Chartrand, S.A. Degterov, G. Eriksson, K. Hack, R.-B. Mahfoud, J. Melançon, A. D. Pelton and S. Petersen, FactSage thermochemical software and databases, *Calphad* 26 (2002) 189-228.
- [2] C.W. Bale, E. Belisle, P. Chartrand, S.A. Dechterov, G. Eriksson, K. Hack, I.-H. Jung, Y.-B. Kang, J. Melançon, A.D. Pelton, C. Robelin and S. Petersen, FactSage thermochemical software and databases - recent developments, *Calphad* 33 (2009) 295-311; www.factsage.com
- [3] A.D. Pelton, S.A. Degterov, G. Eriksson, C. Robelin and Y. Dessureault, The modified quasichemical model I - Binary solutions, *Metall. Mater. Trans. B* 31 (2000) 651~659.
- [4] A.D. Pelton and P. Chartrand, The modified quasichemical model: Part II. multicomponent solutions, *Metall. Mater. Trans. A* 32 (2001) 1355-1360.
- [5] R. Fowler and E. Guggenheim, *Statistical Thermodynamics*, Cambridge University Press, Cambridge, UK (1939).
- [6] A.D. Pelton and M. Blander, Computer assisted analysis of the thermodynamic properties and phase diagrams of slags, *Proc. 2nd Int. Symp. On Metall. Slags and Fluxes, TMS-AIME, Warrendlae, PA* (1984) 281-294
- [7] A. D. Pelton and Y.-B. Kang, Modeling short-range ordering in solutions, *Int. J. of Mat. Res. (formerly Z. Metallk.)* (2007) 907-917.
- [8] M. Hillert, The compound energy formalism, *J. Alloys. Comp.* 320 (2001) 161-176.
- [9] I.-H. Jung, D.-H. Kang, W.-J. Park, N.-J. Kim and S.-H. Ahn, Thermodynamic modeling of the Mg-Si-Sn system, *Calphad* 31 (2007) 192-200.
- [10] A. T. Dinsdale, SGTE data for pure elements, *Calphad* 15 (4) (1991) 317-425.
- [11] F. Jelinek, W. Shickell and B. Gerstein, Thermal study of group II-IV semi conductors - II. heat capacity of Mg₂Sn in the range 5-300K, *J. Phys. Chem. Solids* 28 (1967) 267-270.
- [12] F. Sommer, J.-J. Lee and B. Predel, Temperature dependence of the mixing enthalpies of liquid magnesium-lead and magnesium-tin alloys, *Z. Metallk.* 71 (1980) 818-821.
- [13] S. Fries and H.-L. Lukas, Optimization of the magnesium-tin system, *J. Chim. Phys. et Physico-Chim. Biologique* 90 (1993) 181-187.
- [14] A. Kozlov, M. Ohno, R. Arroyave, Z. Liu and R. Schmid-Fetzer, Phase equilibria, thermodynamics and solidification microstructures of Mg-Sn-Ca alloys, part 1: Experimental investigation and thermodynamic modeling of the ternary Mg-Sn-Ca system,

Intermetallics 16 (2) (2008) 299-315.

- [15] S. Fries and H.-L. Lukas, COST 507 – Thermochemical databases for light metal alloys, Office for Official Publications of the European Communities, Luxembourg, vol. 2, 1998, pp. 81-82.
- [16] P. Chartrand, Thermodynamic optimization of the Al-Mg system, unpublished research, Ecole Polytechnique de Montréal, Canada (2006).
- [17] A. Shukla and A.D. Pelton, Thermodynamic assessment of the Al-Mn and Mg-Al-Mn systems, *J. of Phase Equilibria and Diffusion* 30 (2009) 28-39.
- [18] F. Sommer, N. Rupf-Bolz and B. Predel, Studies on the temperature dependence of the mixing enthalpy of ternary alloy melts., *Z. Metallk.* 74 (1983) 165-171.
- [19] E. Doernberg, A. Kozlov and R. Schmid-Fetzer, Experimental investigation and thermodynamic calculation of Mg-Al-Sn phase equilibria and solidification microstructures, *J. Phase Equilibria and Diffusion* 28 (6) 523-535.
- [20] P. Liang, H.-L. Su, P. Donnadieu, M. G. Harmelin, A. Quivy, P. Ochin, G. Effenberg, H. J. Seifert, H. L. Lukas and F. Aldinger, Experimental investigation and thermodynamic calculation of the central part of the Mg-Al phase diagram, *Z. Metallk.* 89 (1998) 536-540.
- [21] Y.-B. Kang, A.D. Pelton, P. Chartrand and C. D. Fuerst, Critical evaluation and thermodynamic optimization of the Al-Ce, Al-Y, Al-Sc and Mg-Sc binary systems, *Calphad* 32 (2008) 413-422.
- [22] J. Groebner, R. Schmid-Fetzer, A. Pisch, G. Cacciamani, P. Riani, N. Parodi, G. Borzone, A. Saccone and R. Ferro, Experimental investigations and thermodynamic calculation in the Al-Mg-Sc system, *Z Metallk.* 90 (1999) 872-880.
- [23] A. Pisch, R. Schmid-Fetzer, G. Cacciamani, P. Riani, A. Saccone and R. Ferro, Mg-rich phase equilibria and thermodynamic assessment of the Mg-Sc system, *Z. Metallkd.* 89 (1998) 474-477.
- [24] M. Kawakami, A further investigation of the heat of mixture in molten metals, *Sci. Rep. Res. Inst. Tohoku Univ.* 19 (1930) 521-549.
- [25] A. Nayak and W. Oelsen, Determination of the heats of formation of the solid and liquid Mg-Sn alloys at 20° and 800°C respectively and the heat content of the alloys at 800°C, *Trans. Indian Inst. of Metals* 24 (1971) 66-73.
- [26] C. Eckert, R. Irwin and J. Smith, Thermodynamic activity of magnesium in several highly-solvating liquid alloys, *Metall. Mater. Trans. B* 14 (1983) 451-458.
- [27] Z. Moser, W. Zakulski, Z. Panek, M. Kucharski and L. Zabdyr, Thermodynamic study and

- the phase diagram of the Mg-Sn system, *Metall. Mater. Trans. B* 21 (1990) 707-714.
- [28] J. Egan, Thermodynamics of liquid magnesium alloys using CaF₂ solid electrolytes, *J. Nuclear Mat.* 51 (1974) 30-35.
- [29] R. A. Sharma, Thermodynamic properties of liquid Mg+Pb and Mg+Sn alloys by e.m.f. measurements, *J. Chem. Thermo.* 2 (1970) 373-389.17
- [30] N. Kurnakow and N. Stepanow, On the alloys of magnesium with tin and thallium, *Z. Anorg. Chem.* 46 (1905) 177-192.
- [31] G. Grube, On the alloys of magnesium with tin and thallium, *Z. Anorg. Chem.* 46 (1905) 76-84.
- [32] G. Raynor, The constitution of the magnesium-rich alloys in the systems magnesium-lead, magnesium-tin, magnesium-germanium, and magnesium-silicon, *J. Inst. Met.* 6 (1940) 403-426.
- [33] W. Hume-Rothery, The system magnesium-tin and the compound Mg₄Sn₂, *J. Inst. Met.* 35 (1926) 336-347.
- [34] J. Ellmer, K. Hall, R. Kamphenfner, J. Pfeifer, V. Stamboni and C. Graham, On the liquidus in tin-rich Sn-Mg alloys, *Metall. Trans.* 4 (1973) 889-891.
- [35] A. Nayak and W. Oelsen, Thermal analysis of Mg-Sn alloys by calorimetric measurements for determination of the liquidus curve (part 1), *Trans. Indian Inst. Met.* (1968) 15-20.
- [36] C. Heycock and F. Neville, The molecular weights of metals when in solution, *J. Chem. Soc.* 57 (1890) 376-392.
- [37] A. Steiner, E. Miller and K. Komarek, Magnesium-tin phase diagram and thermodynamic properties of liquid magnesium-tin alloys, *Trans. Metall. Soc. AIME* 230 (1964) 1361-1367.
- [38] G. Grube and H. Vosskuhler, Electrical conductivity and binary alloys phase diagram, *Z. Electrochem.* 40 (1934) 566-570.
- [39] L. Willey, unpublished research, Aluminum Research Laboratories, See *Metals Handbook*, 1948 ed., The American Society for Metals, Cleveland, OH 1227 (1948).
- [40] H. Vosskuhler, Solubility of tin in magnesium, *Metallwirtschaft* 245 (1941) 805-808.
- [41] A. Nayak and W. Oelsen, Quantitative thermal analysis of magnesium-tin alloys by calorimetric measurement for the determination of solidus and liquidus curves, *Trans. Indian Inst. Met.* (1969) 53-58.
- [42] A. Gwyner, Al-Bi and Al-Sn alloys, *Z. Anorg. Chem.* 49 (1906) 311-316.

- [43] A. Sully, H. Hardy and T. Heal, The Al-Sn phase diagram and the characteristics of Al alloys containing Sn as an alloying element, *J. Inst. Met.* 76 (1949) 269-294.
- [44] E. Bonnier, F. Durand and G. Massart, Thermodynamic study of the system Al-Sn, *C.R. Acad. Sci. Paris* 259 (1964) 380-383.
- [45] L. Samuels, The solid solubilities of Sn, In, and Cd in Al, *J. Inst. Met.* 84 (1955) 333-336.
- [46] R. Dorward, The solubility of tin in aluminum, *Metall. Mater. Transactions A* 7 (1976) 308-310.
- [47] A. Campbell and R. Kartzmark, The systems aluminum-tin and aluminum-lead-tin, *Canadian J. Chem.* 34 (1956) 1428-1439.
- [48] F. Wittig and G. Keil, Heats of mixing of liquid Al with Zn, Cd, In, Th, Sn, Pb, and Bi, *Z. Metallkd.* 54 (1963) 576-590.
- [49] W. Oelsen, P. Zuhlke and O. Oelsen, Thermodynamic analysis. XII: automatic recording of heat content vs reciprocal absolute temperature, *Arch. Eisenhüttenwes* 29 (1958) 799-805.
- [50] T. Badaeva and R. Kuznetsova, Structure of aluminum with magnesium and tin, *Trudy Inst. Met.* (1958) 203-215.
- [51] Liquidus determinations of polynary magnesium alloys, Tech. rep., Dow Chemicals, Office of Naval Res., Final Status Report No. 15004, Contract No. N9 ONR 85900 (1950), cited in Ref. [19].
- [52] E. Semenova, Magnesium-aluminum-tin phase diagram in the magnesium-rich phase, *Doklady Akademii Nauk SSSR* 188 (1969) 1308-1310.
- [53] N. Turkina and V. Kuz'mina, Phase reactions in Al-Mg-Sc alloys (up to 26% Mg and 3% Sc), *Russ. Metall.* (1976) 179-183.
- [54] C. Robelin, P. Chartrand, and A. D. Pelton, Thermodynamic evaluation and optimization of the (NaCl + KCl + AlCl₃) system, *The Journal of Chemical Thermodynamics* 36, (2004) 683-699.
- [55] W. Fischer and A.-L. Simon, The Thermal Properties of Halides. 15. The Melting Diagram of the System AlCl₃-NaCl-KCl, with Observations on the the Electrolysis of Na-Al-Cl Melts, *Z. Anorg. Allg. Chem.* (1960) 1-12.

Table 1. Model parameters of the Mg-Al-Sn and Mg-Al-Sc systems optimized in the present study (J/mol). Major species in each sublattice are in bold.

Liquid [‡]					
Coordination Numbers [†]				Gibbs energies of pair exchange reactions (J/mole of pairs)	
<i>i</i>	<i>j</i>	Z_{ij}^i	Z_{ij}^j		
Mg	Sn	4	8	Δg_{MgSn}	$= -15,271.6 - 0.8786T + (3,347.2 + 0.4184T)X_{\text{MgMg}}$
Al	Sn	6	6	Δg_{AlSn}	$= 5,439.2 - 1.8830T + (2,510.4 - 0.4184T)X_{\text{AlAl}} + (-836.8 + 0.8368T)X_{\text{SnSn}}$
Al	Mg	6	6	Δg_{AlMg}	$= -2761.44 + 1.5272T + (-418.4 + 0.6276T)X_{\text{AlAl}}$ (from reference [16, 17])
(Al,Mg) ₃ Sc					
$G_{\text{Al:Sc}}$	$= G^{\circ}_{\text{Al}_3\text{Sc}}$ from reference [27]				
$G_{\text{Mg:Sc}}$	$= 3 \times G(\text{Mg,HCP}) + G(\text{Sc,HCP}) - 12,552$				
$L_{\text{Al,Mg:Sc}}$	$= -37,656$				
HCP: (Mg, Al, Sn)					
$L_{\text{Al,Mg}}$	$= 2,510.4$ (from reference [16])				
$L_{\text{Mg,Sn}}$	$= -48,116(X_{\text{Mg}} - X_{\text{Sn}})$				
FCC: (Al, Mg)					
$L_{\text{Al,Mg}}$	$= 4,144.03 - 4.3793T + (-207.44 + 3.0546T)(X_{\text{Al}} - X_{\text{Mg}})$ (from reference [16])				
BCT: (Sn, Al)					
$L_{\text{Al,Sn}}$	$= 14136.95 - 4.7123T$ (from reference [15])				
(Al, Mg)[Sc, Mg] [‡]					
$G_{\text{Al:Sc}}$	$= G^{\circ}_{\text{AlSc}}$ from reference [27]				
$G_{\text{Al:Mg}}$	$= G(\text{Al,FCC}) + G(\text{Mg,HCP}) + 41,840$				
Mg ₂ Sn					
$G^{\circ}_{\text{Mg}_2\text{Sn}}$	$= -102589.83 + 367.50166T - 68.331T \ln T - 0.0178986T^2 + 3.33829 \times 10^{-7}T^3 - 95970/T$				

[†] For all pure elements (Al, Mg, Sc and Sn), $Z_{ii}^i = 6$

[‡] All other parameters are given in Reference [21].

Figure Captions

- Figure 1: Enthalpy of mixing in Mg-Sn liquid alloys as optimized by the MQM or the associate model compared to experimental data [12, 24, 25].
- Figure 2: Entropy of mixing in Mg-Sn liquid alloys at 800°C calculated from the optimizations using the MQM or the associate model.
- Figure 3: Partial excess Gibbs energies of mixing in Mg-Sn alloys at 800°C as optimized by the MQM or the associate model compared to experimental data [26-29].
- Figure 4: Calculated liquidus projection of the Mg-Al-Sn system using the MQM for the liquid phase. Temperatures in °C.
- Figure 5: Phase diagram of the Mg-Sn system as optimized using the MQM or the associate model for the liquid phase compared to experimental data [30-41].
- Figure 6: Phase diagram of the Al-Sn system optimized using the MQM for the liquid phase compared to experimental data [42-47].
- Figure 7: Enthalpy of mixing in Al-Sn liquid alloys as optimized by the MQM compared to experimental data [24,48,49].
- Figure 8: Optimized phase diagram of the Mg-Al system [16].
- Figure 9: Calculated section of the Mg-Al-Sn system along the $\text{Mg}_{0.6667}\text{Sn}_{0.3333}\text{-Al}$ ($\text{Mg}_2\text{Sn-Al}$) join using the MQM (with no ternary parameters), or the associate model without ternary parameters, or the associate model with a ternary parameter, compared to experimental data [19, 50].
- Figure 10: Calculated section of the Mg-Al-Sn system along the $\text{Mg}_{0.9777}\text{Sn}_{0.0223}\text{-Al}$ join using the MQM (with no ternary parameters), or the associate model without ternary parameters, or the associate model with a ternary parameter, compared to experimental data [50].
- Figure 11: Calculated sections of Mg-Al-Sn system using the MQM (with no ternary parameters) for the liquid phase, compared to experimental data [19] (Δ, ∇), [50] (\circ), [51](\diamond), [52](\square).
- Figure 12: Calculated enthalpy of mixing in the Mg-Al-Sn liquid alloy along the (a) $\text{Mg}_{0.6667}\text{Sn}_{0.3333}\text{-Al}$, (b) $\text{Mg}_{0.5}\text{Sn}_{0.5}\text{-Al}$, and (c) $\text{Mg}_{0.3}\text{Sn}_{0.7}\text{-Al}$ joins using the MQM (with no ternary parameters), or the associate model without ternary parameters, or the associate model with a ternary parameter, compared to experimental data [18].
- Figure 13: Calculated enthalpy of mixing of Mg-Al-Sn liquid alloy along the $\text{Mg}_{0.5}\text{Al}_{0.5}\text{-Sn}$ section using the MQM (with no ternary parameters), or the associate model without

ternary parameters, or the associate model with a ternary parameter, compared to experimental data [18].

- Figure 14: Calculated liquidus projection of the Mg-Al-Sc system using the MQM (with no ternary parameters) for the liquid phase. Temperatures in °C.
- Figure 15: Calculated isothermal section of the Mg-Al-Sc system at 350°C compared with experimental data [22].
- Figure 16: Calculated section of the Mg-Al-Sc system along the $\text{Al}_{0.6667}\text{Sc}_{0.3333}$ -Mg (Al_2Sc -Mg) join using the MQM (with no ternary parameters), or the associate model without ternary parameters, compared to experimental data [19, 50].
- Figure 17: Calculated sections of the Mg-Al-Sc system along the (a) (Al-22wt%Mg)-(Al-2wt%Sc), (b) (Al-17wt%Mg)-(Al-1wt%Sc) joins compared with experimental data [53].
- Figure 18: Calculated section of the Mg-Al-Sc system at $X_{\text{Mg}} = 0.36$ compared with experimental data [22].
- Figure 19: Calculated [54] liquidus projection of the (NaCl + KCl + AlCl_3) system (the calculated isobar at 0.1MPa is shown).
- Figure 20: Calculated (NaCl + KAlCl_4) quasibinary phase diagram compared with experimental data [55].

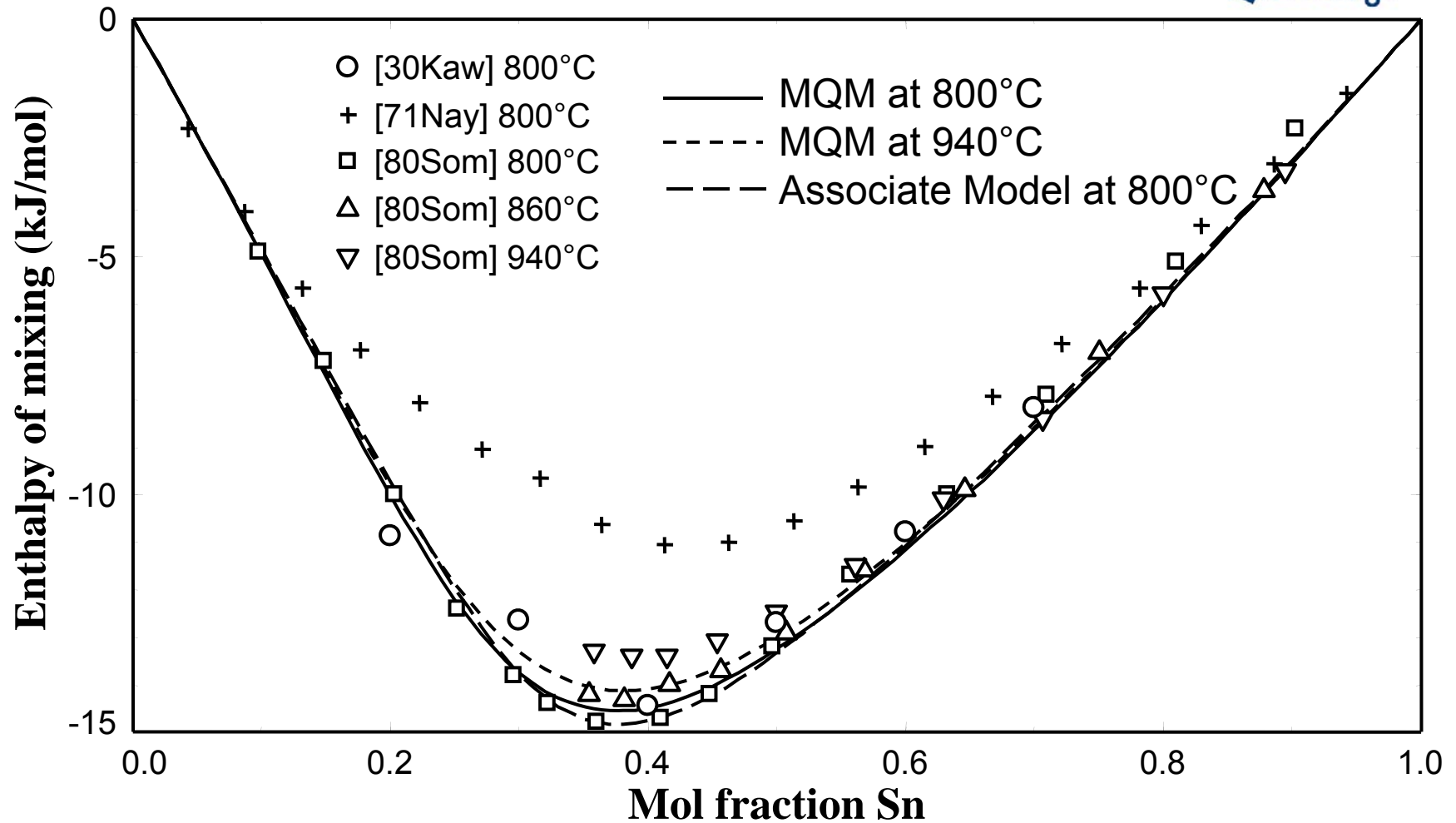


Figure 1: Enthalpy of mixing in Mg-Sn liquid alloys as optimized by the MQM or the associate model compared to experimental data [12, 24, 25].

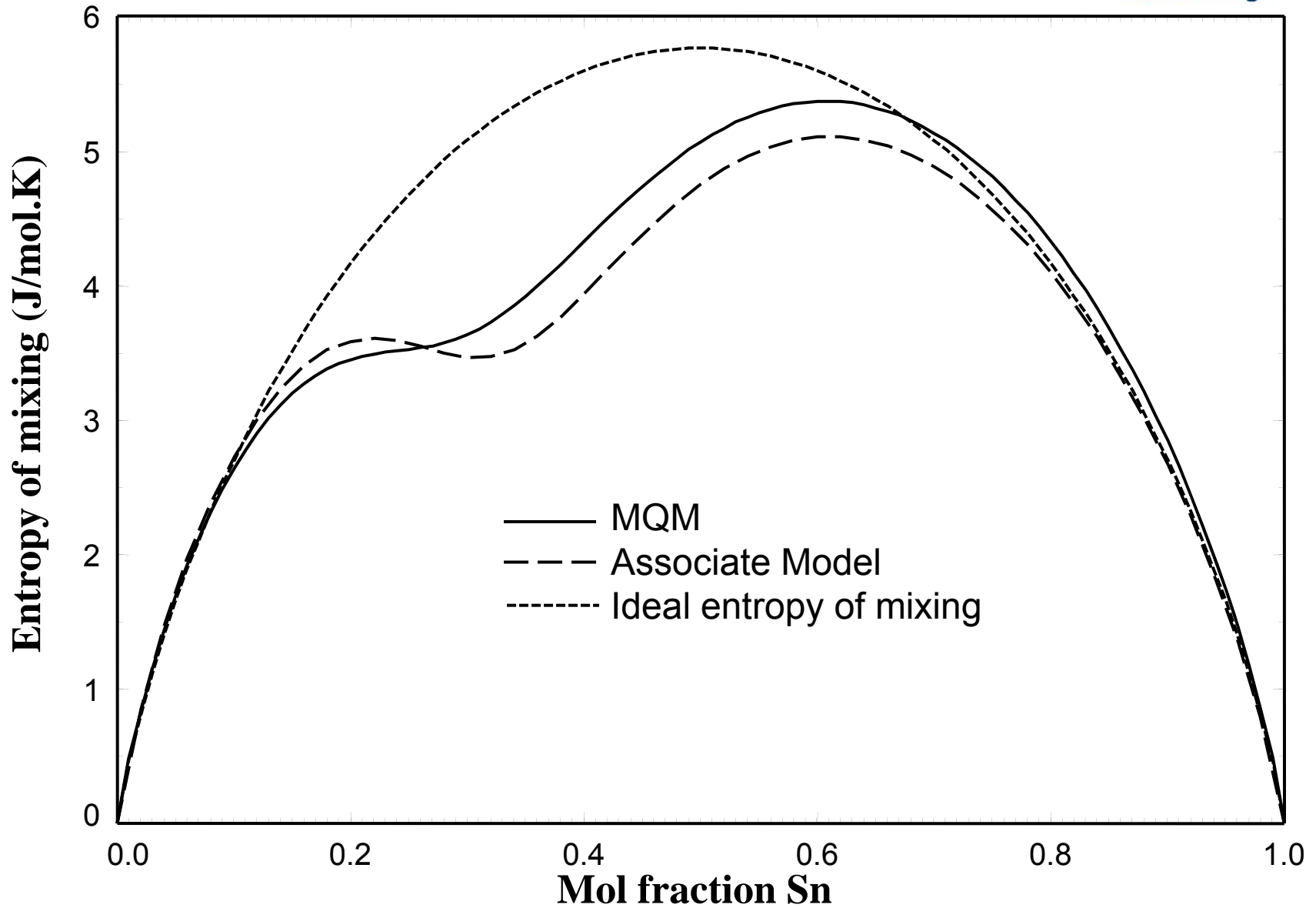


Figure 2: Entropy of mixing in Mg-Sn liquid alloys at 800°C calculated from the optimizations using the MQM or the associate model.

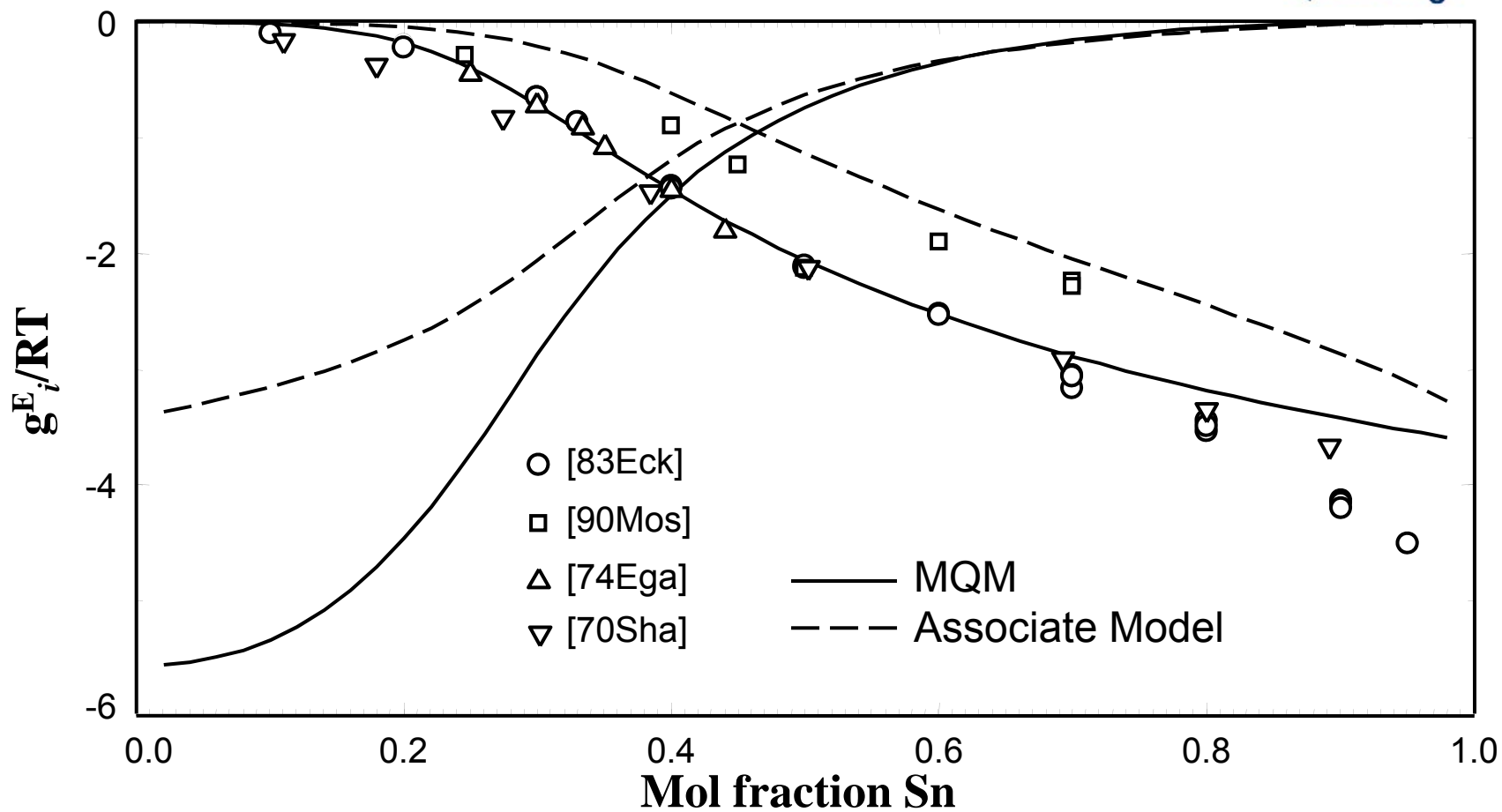


Figure 3: Partial excess Gibbs energies of mixing in Mg-Sn alloys at 800°C as optimized by the MQM or the associate model compared to experimental data [26-29].

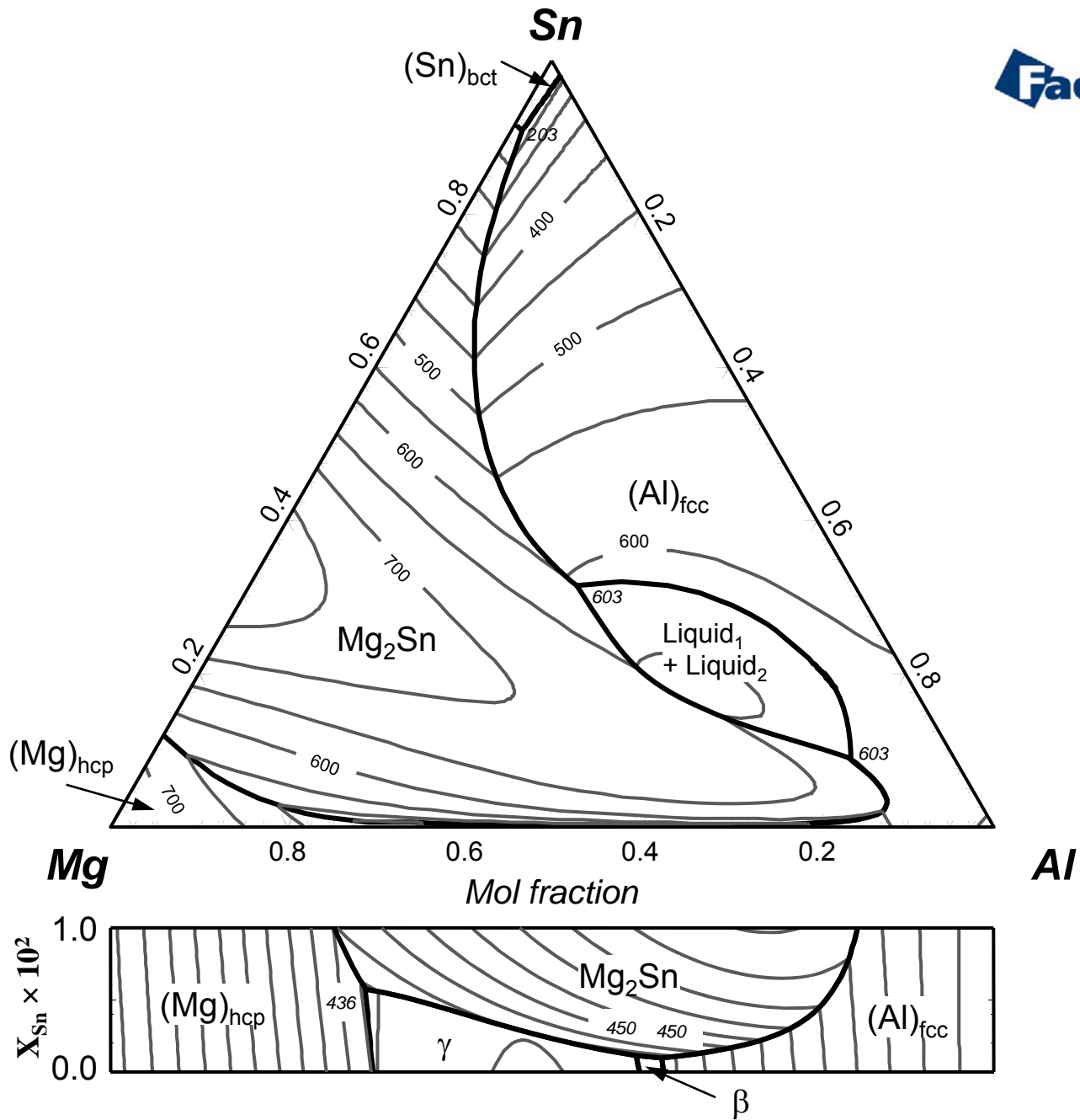


Figure 4: Calculated liquidus projection of the Mg-Al-Sn system using the MQM for the liquid phase. Temperatures in °C.

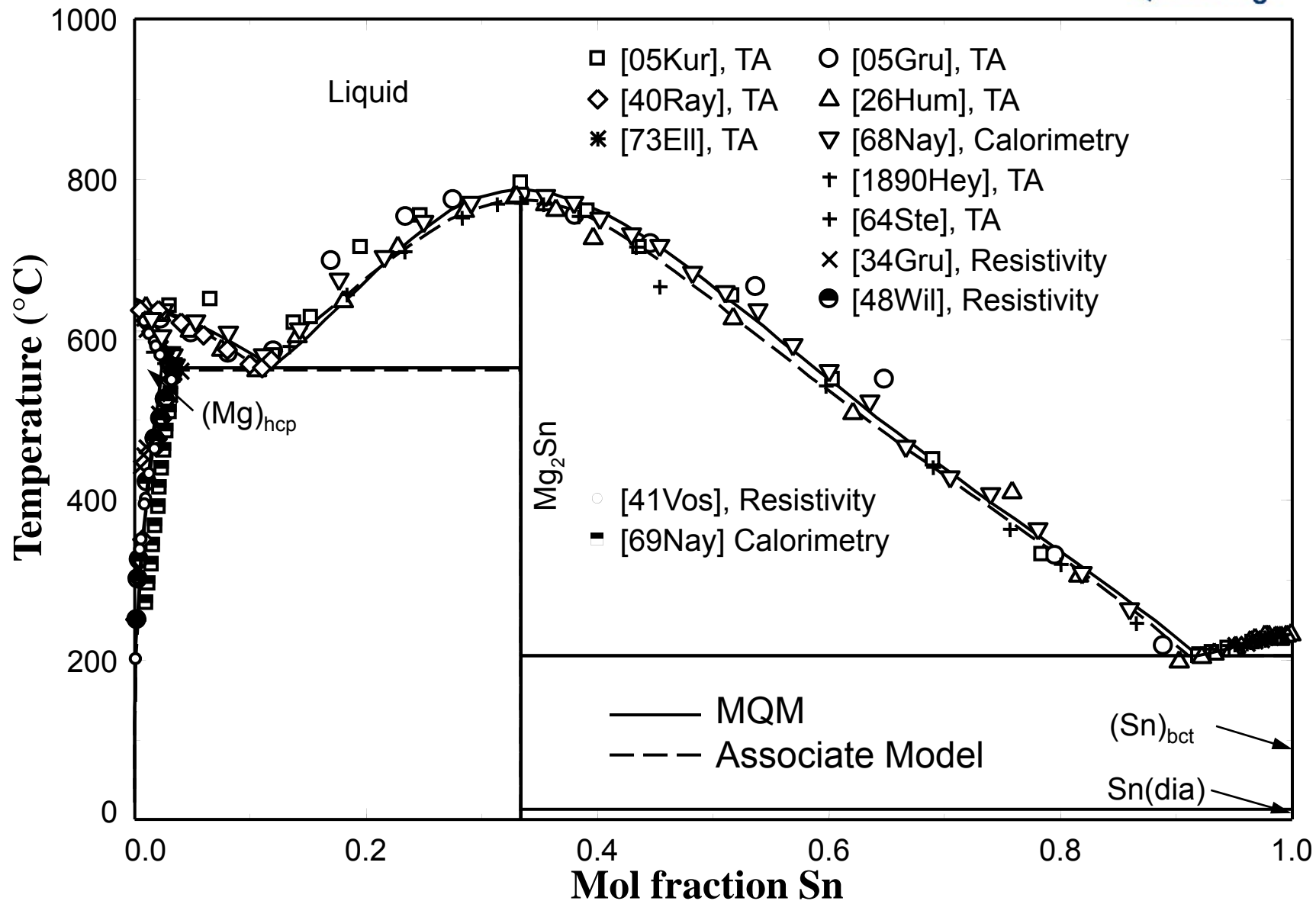


Figure 5: Phase diagram of the Mg-Sn system as optimized using the MQM or the associate model for the liquid phase compared to experimental data [30-41].

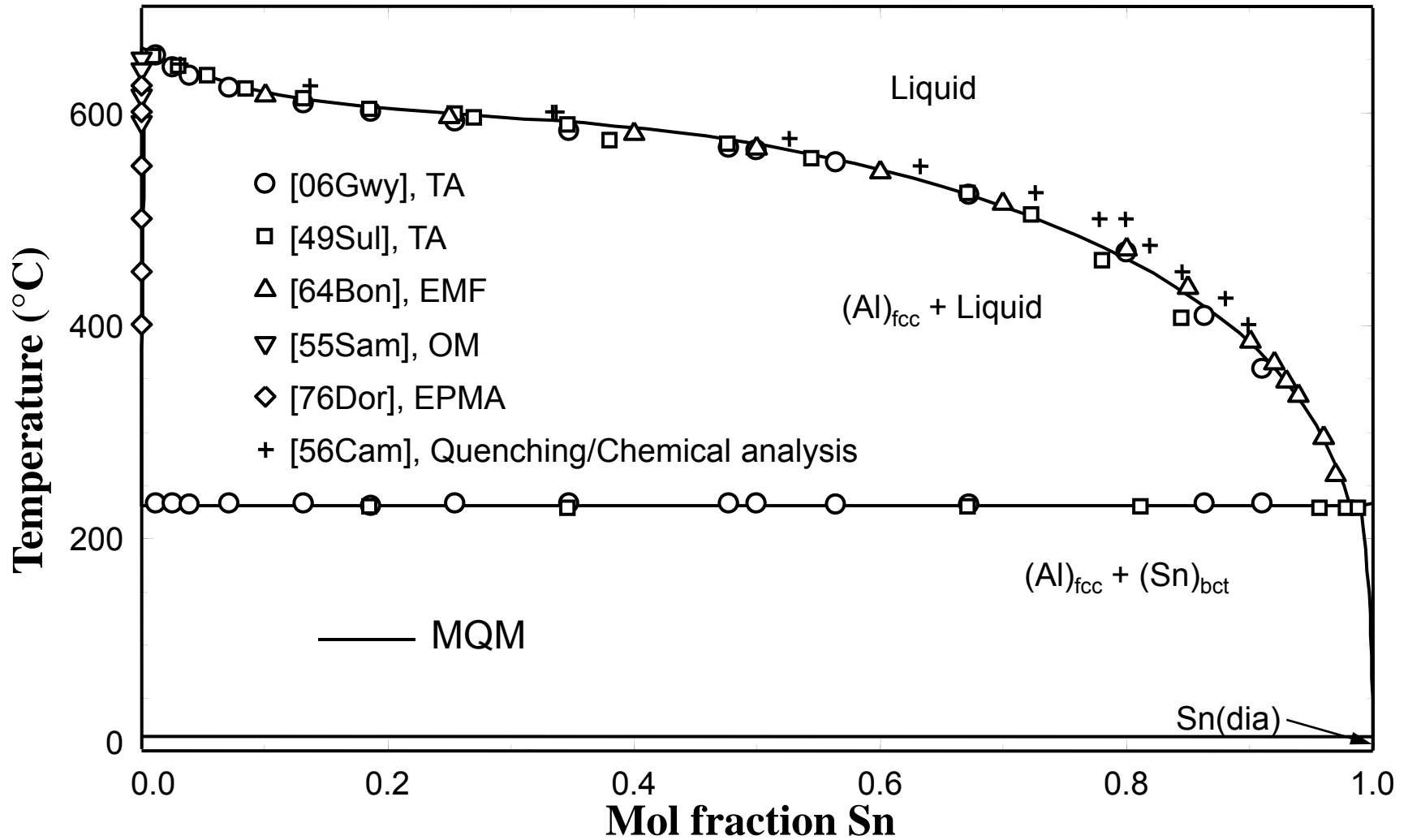


Figure 6: Phase diagram of the Al-Sn system optimized using the MQM for the liquid phase compared to experimental data [42-47].

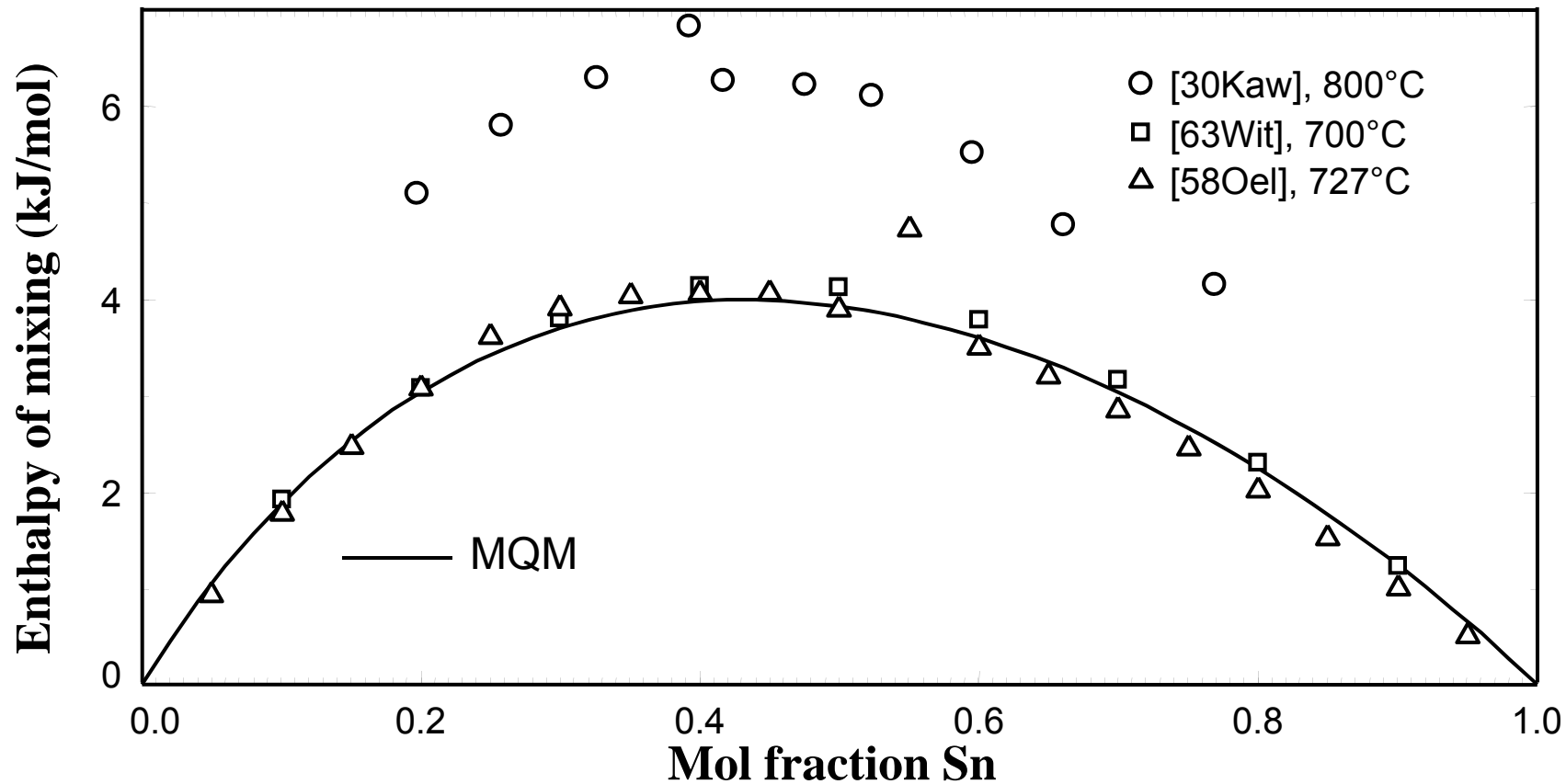


Figure 7: Enthalpy of mixing in Al-Sn liquid alloys as optimized by the MQM compared to experimental data [24,48,49].

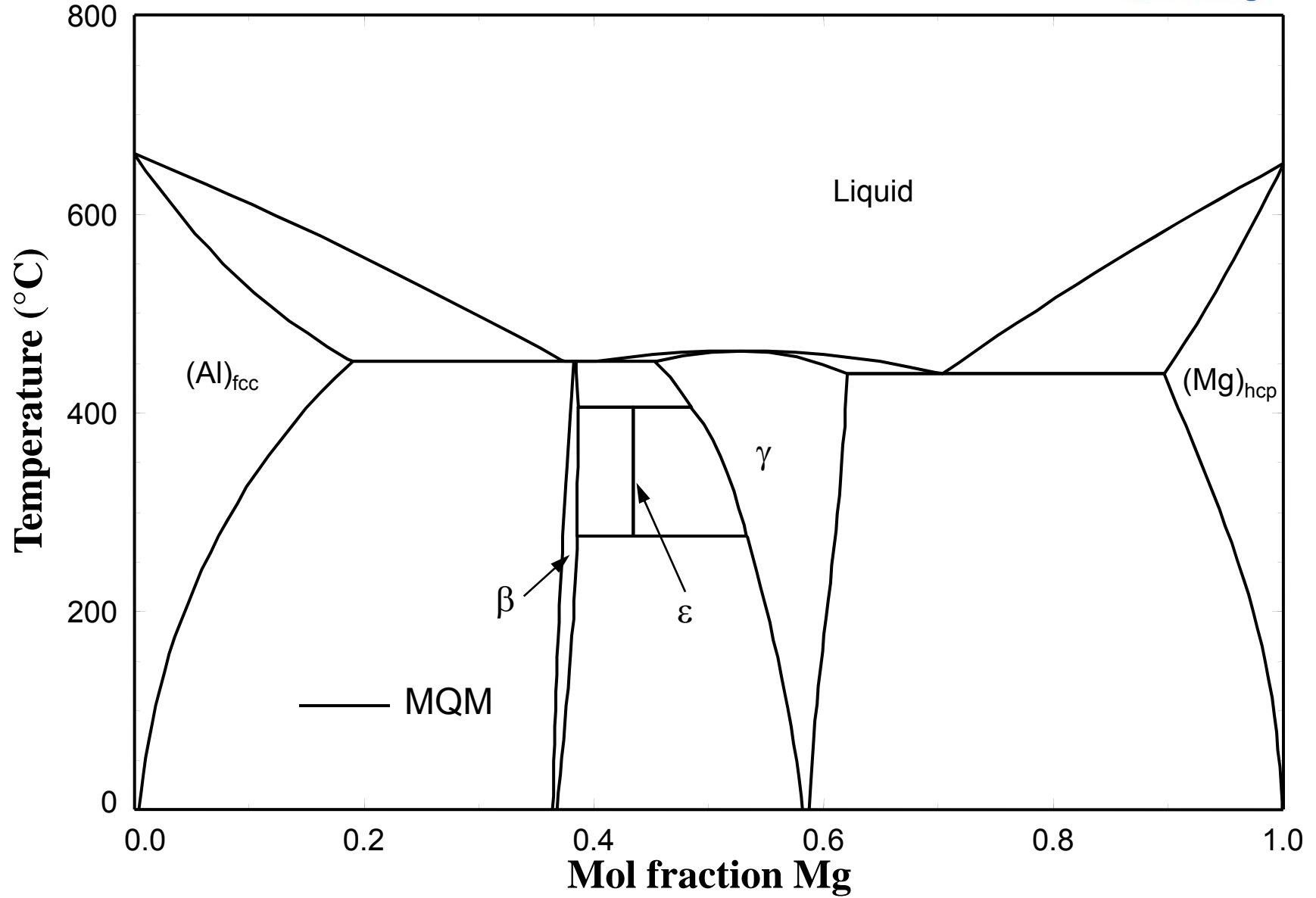


Figure 8: Optimized phase diagram of the Mg-Al system [16].

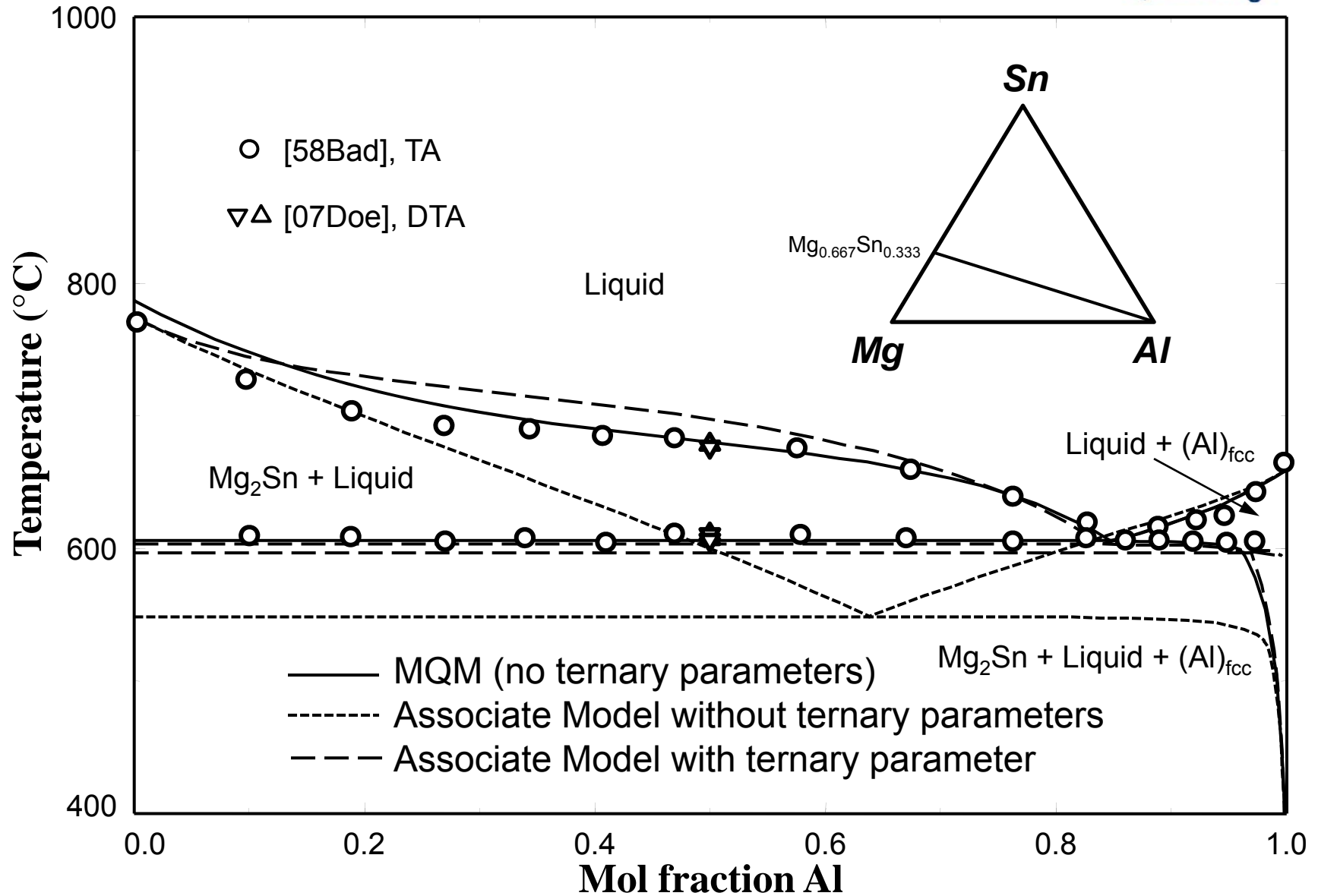


Figure 9: Calculated section of the Mg-Al-Sn system along the Mg_{0.6667}Sn_{0.3333}-Al (Mg₂Sn-Al) join using the MQM (with no ternary parameters), or the associate model without ternary parameters, or the associate model with a ternary parameter, compared to experimental data [19, 50].

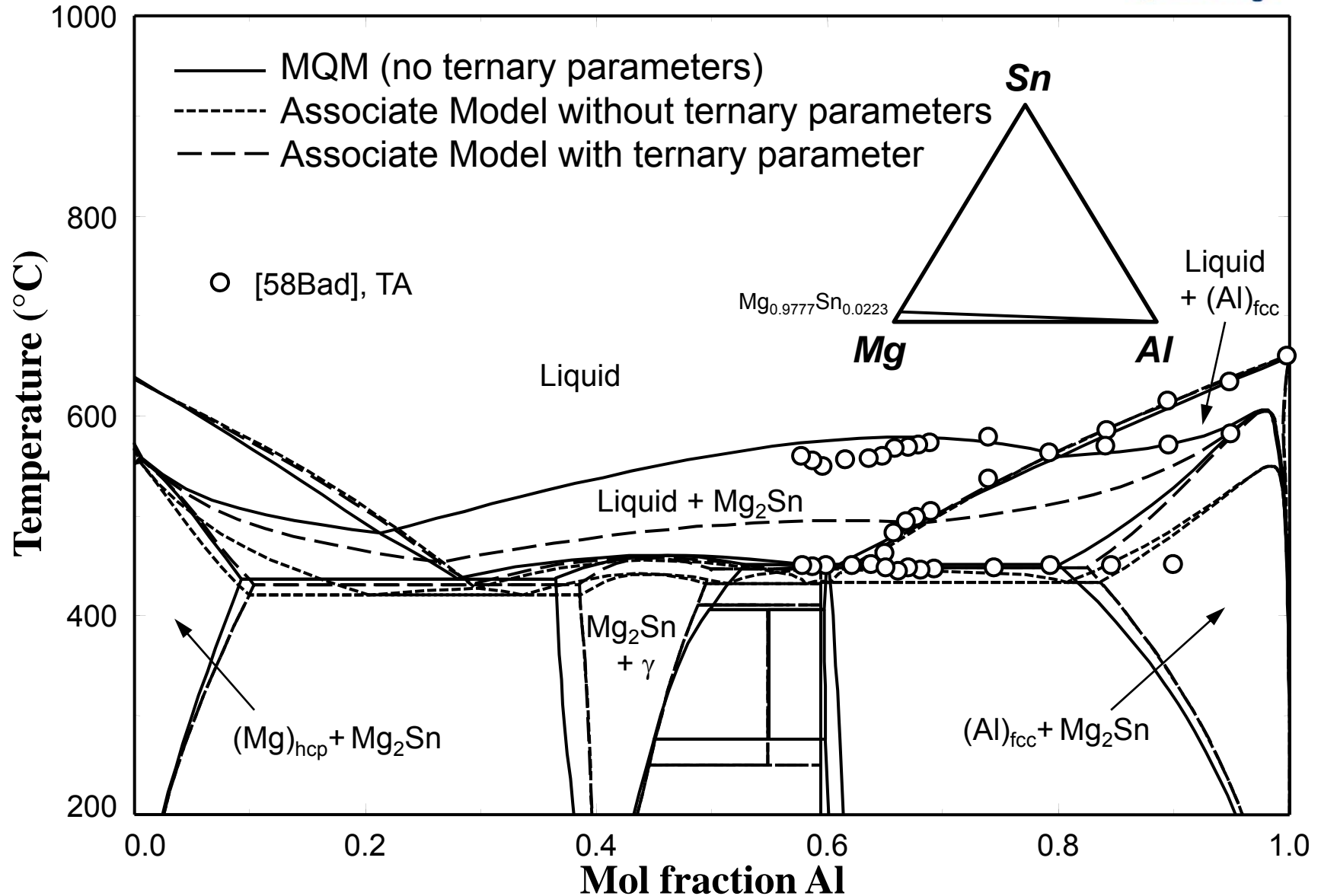


Figure 10: Calculated section of the Mg-Al-Sn system along the $Mg_{0.9777}Sn_{0.0223}$ -Al join using the MQM (with no ternary parameters), or the associate model without ternary parameters, or the associate model with a ternary parameter, compared to experimental data [50].

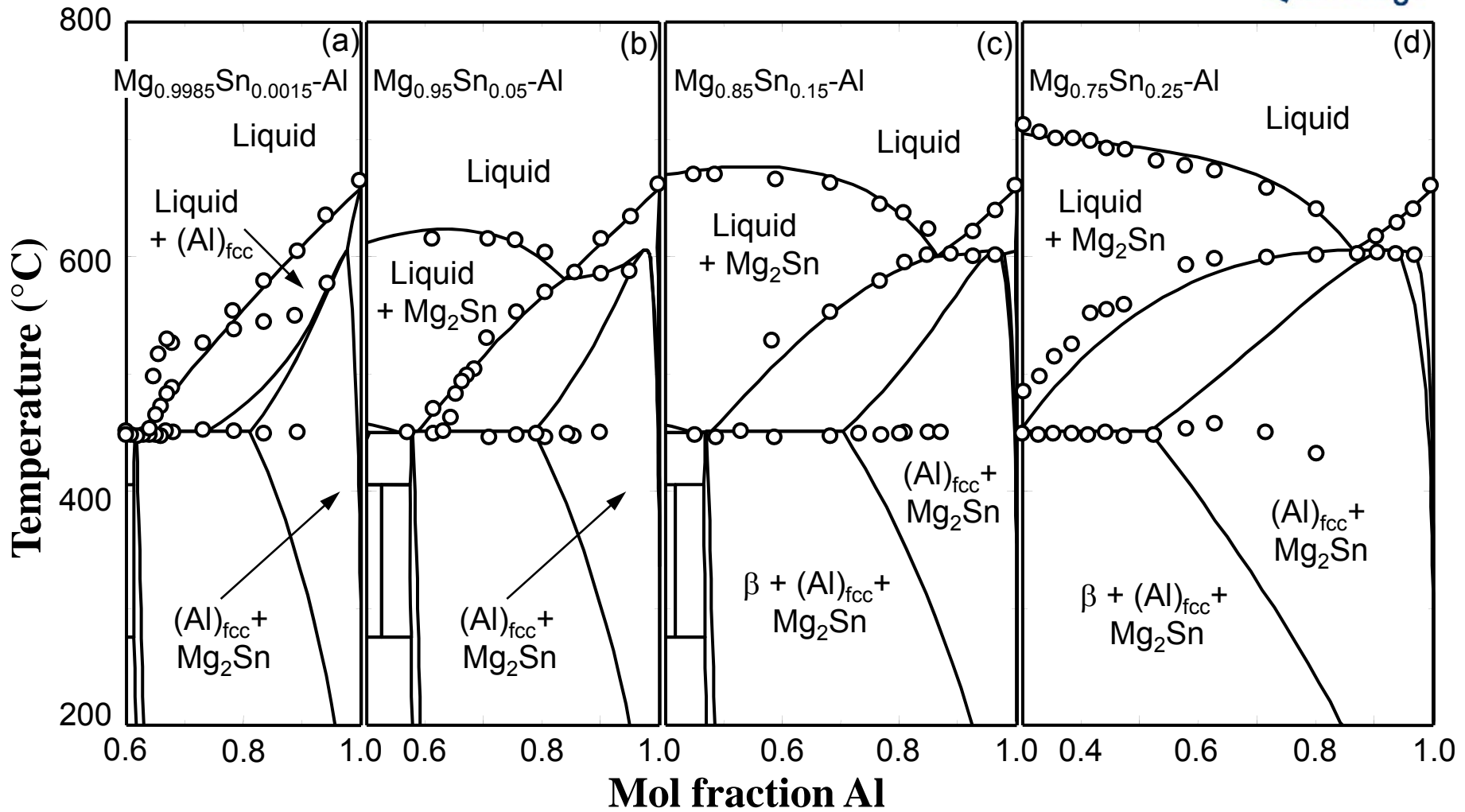


Figure 11: Calculated sections of Mg-Al-Sn system using the MQM (with no ternary parameters) for the liquid phase, compared to experimental data [19] (Δ, ∇), [50] (\circ), [51] (\diamond), [52] (\square).

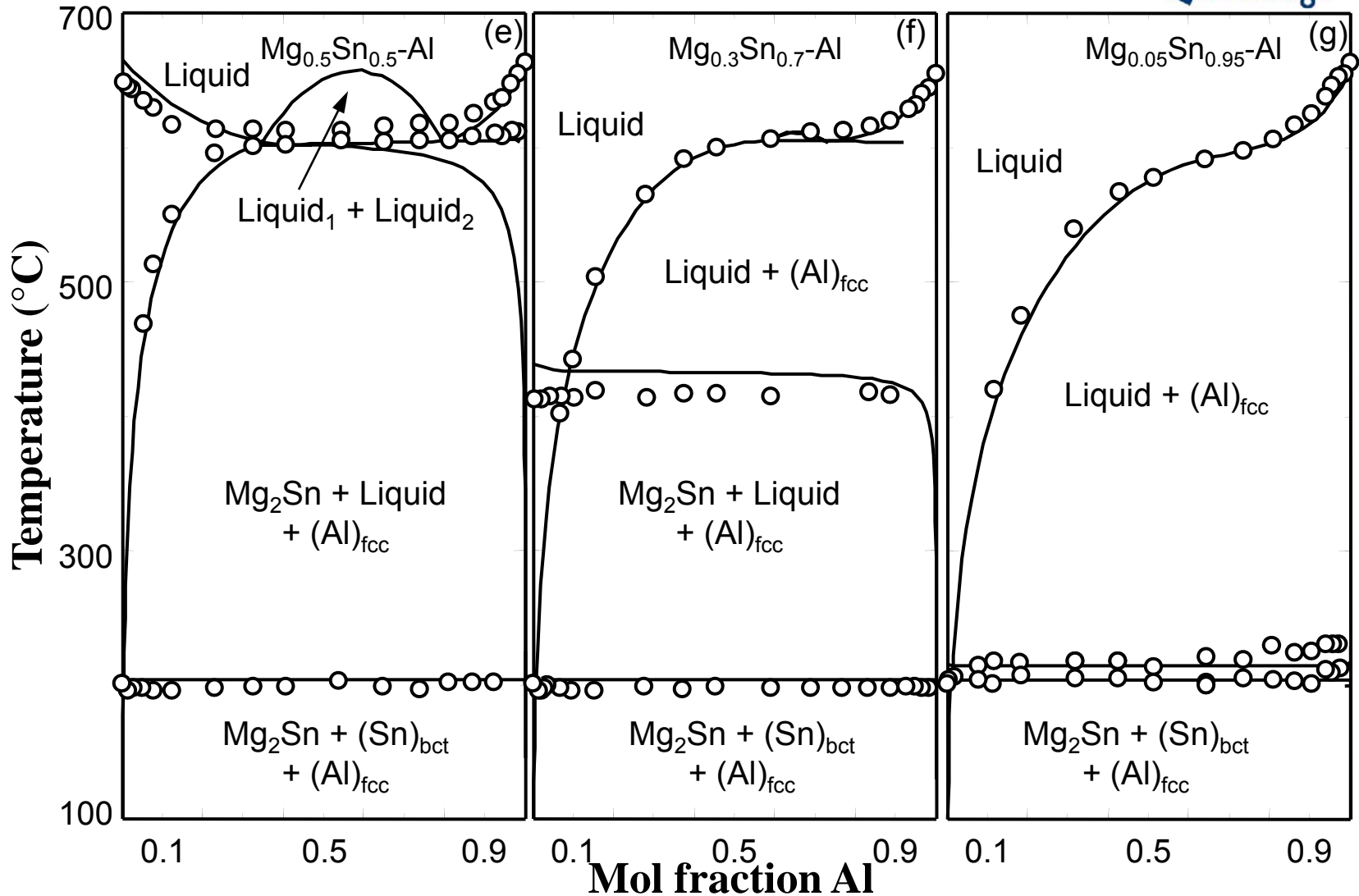


Figure 11: Calculated sections of Mg-Al-Sn system using the MQM (with no ternary parameters) for the liquid phase, compared to experimental data [19] (Δ, ∇), [50] (\circ), [51] (\diamond), [52] (\square).

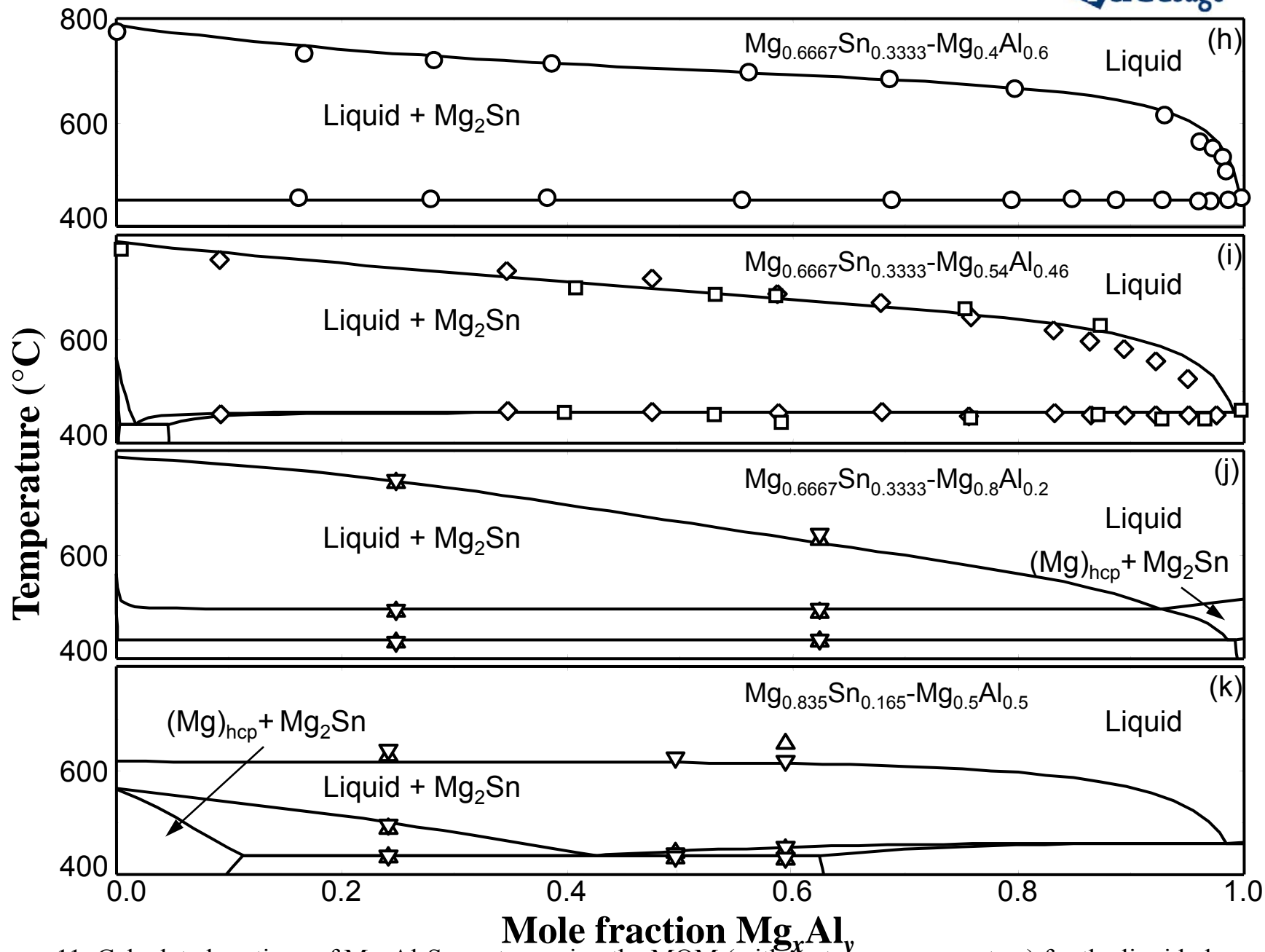


Figure 11: Calculated sections of Mg-Al-Sn system using the MQM (with no ternary parameters) for the liquid phase, compared to experimental data [19] (Δ, ∇), [50] (\circ), [51] (\diamond), [52] (\square).

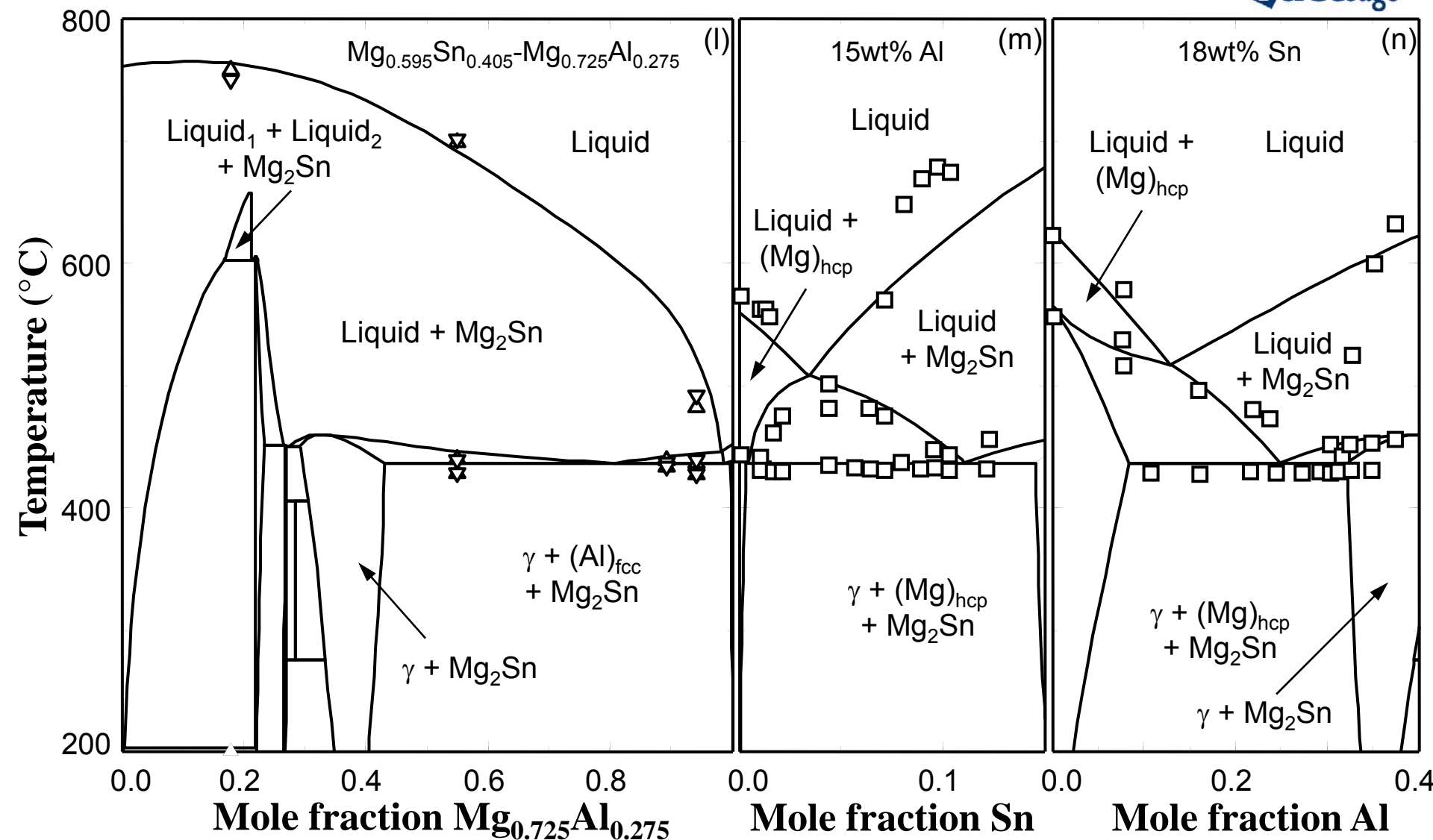


Figure 11: Calculated sections of Mg-Al-Sn system using the MQM (with no ternary parameters) for the liquid phase, compared to experimental data [19] (Δ, ∇), [50] (\circ), [51] (\diamond), [52] (\square).

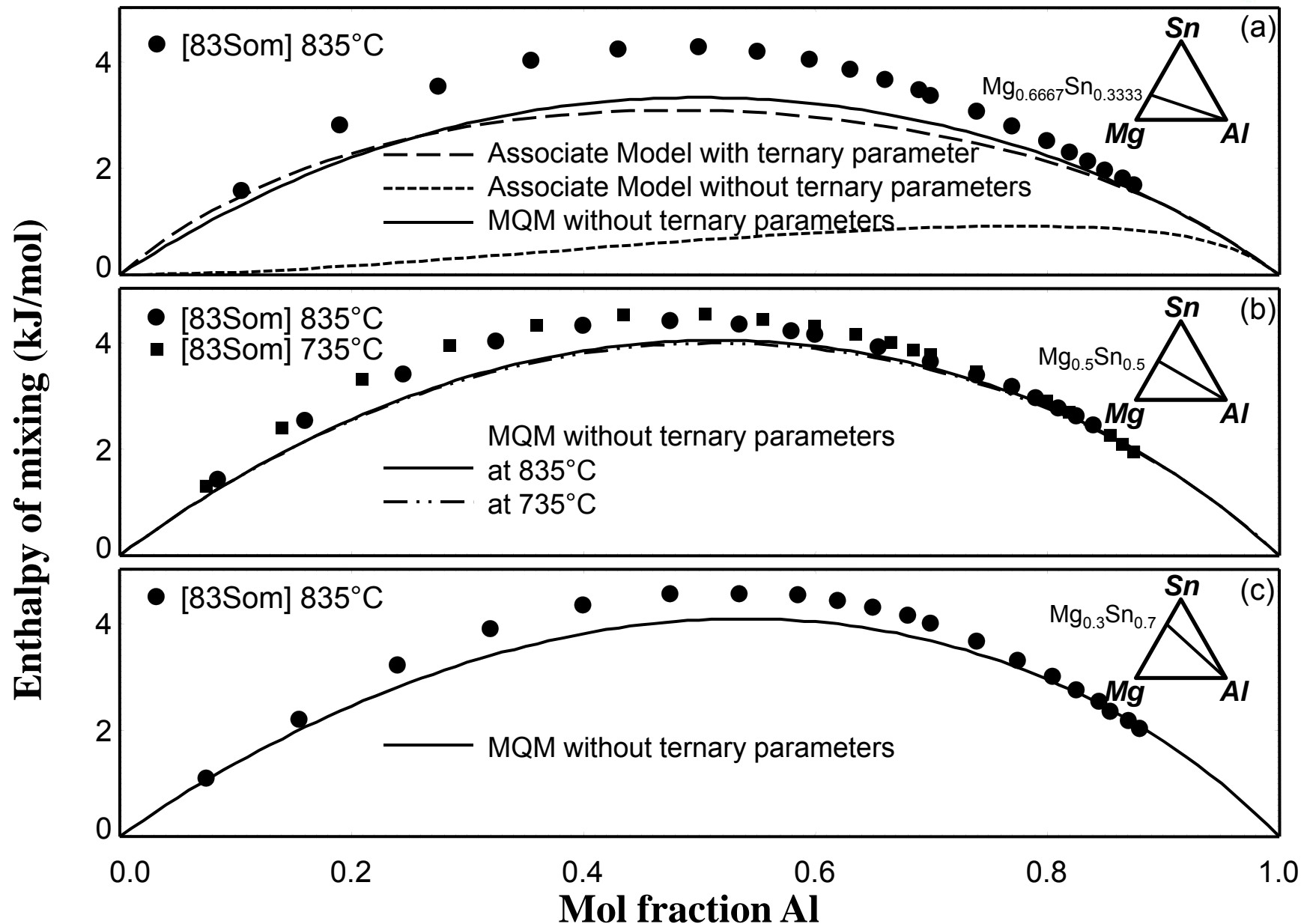


Figure 12: Calculated enthalpy of mixing in the Mg-Al-Sn liquid alloy along the (a) Mg_{0.6667}Sn_{0.3333}-Al, (b) Mg_{0.5}Sn_{0.5}-Al, and (c) Mg_{0.3}Sn_{0.7}-Al joins using the MQM (with no ternary parameters), or the associate model without ternary parameters, or the associate model with a ternary parameter, compared to experimental data [18].

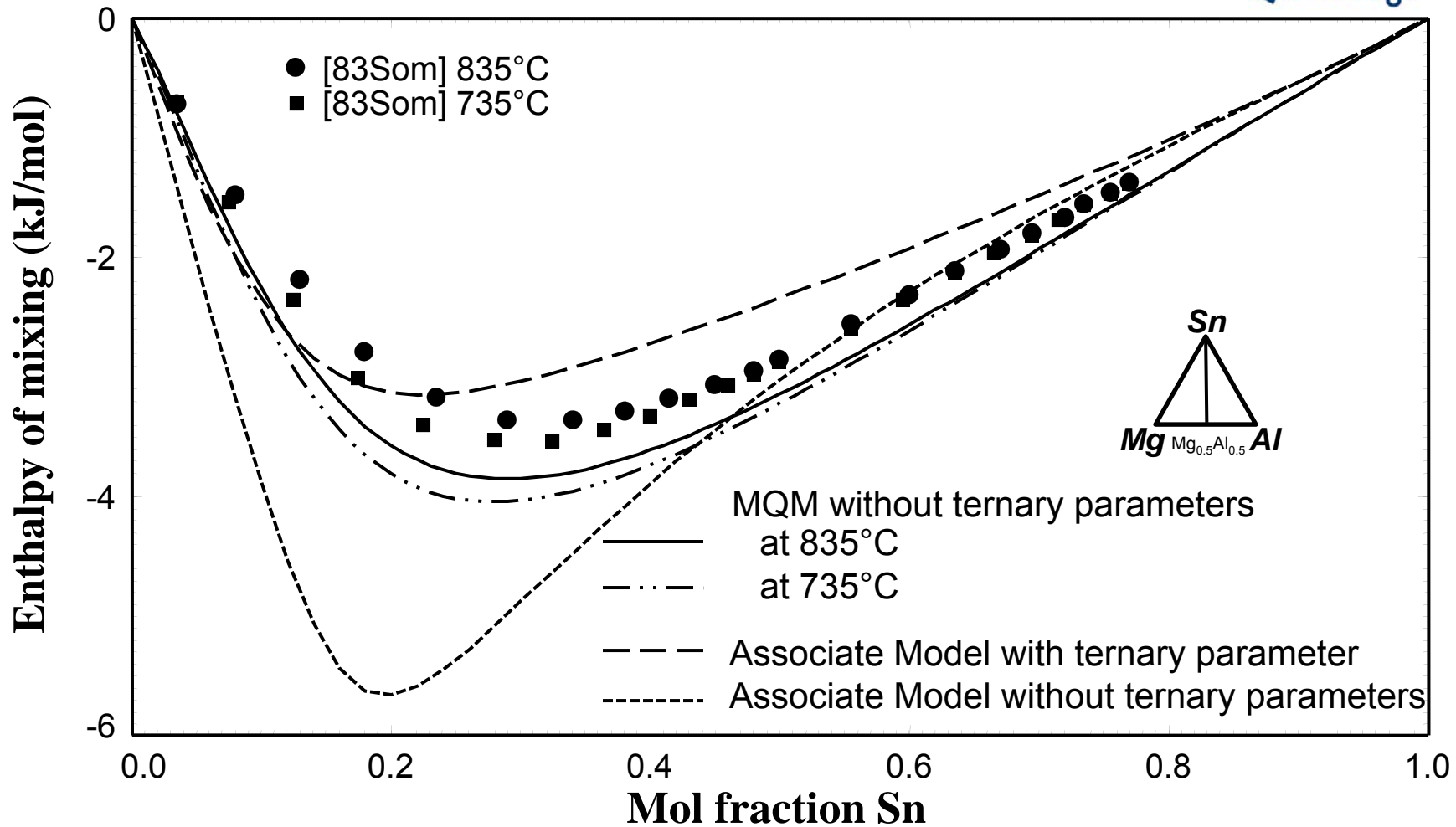


Figure 13: Calculated enthalpy of mixing of Mg-Al-Sn liquid alloy along the $Mg_{0.5}Al_{0.5}$ -Sn section using the MQM (with no ternary parameters), or the associate model without ternary parameters, or the associate model with a ternary parameter, compared to experimental data [18].

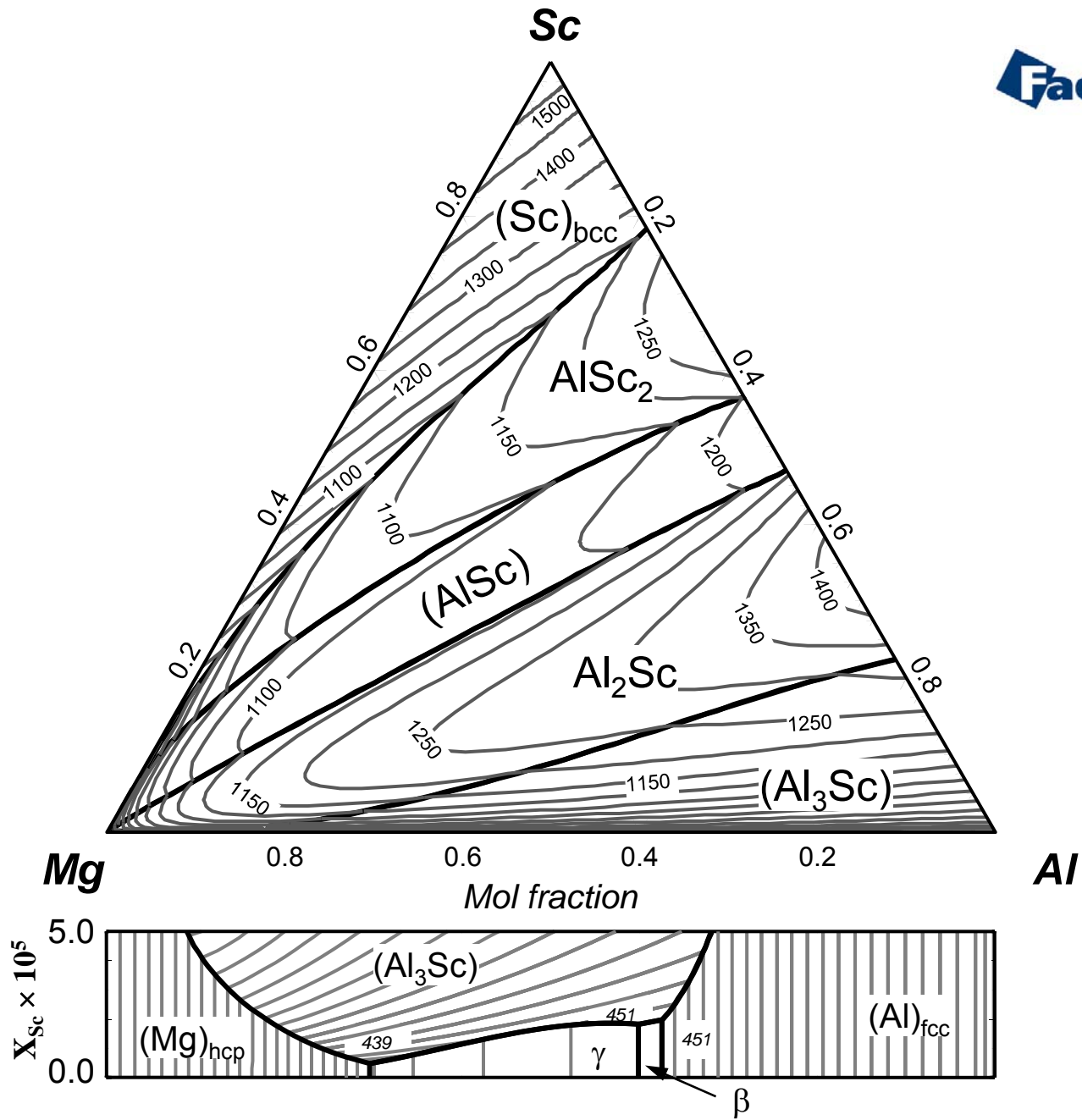


Figure 14: Calculated liquidus projection of the Mg-Al-Sc system using the MQM (with no ternary parameters) for the liquid phase. Temperatures in °C.

[99Gro] T = 350°C

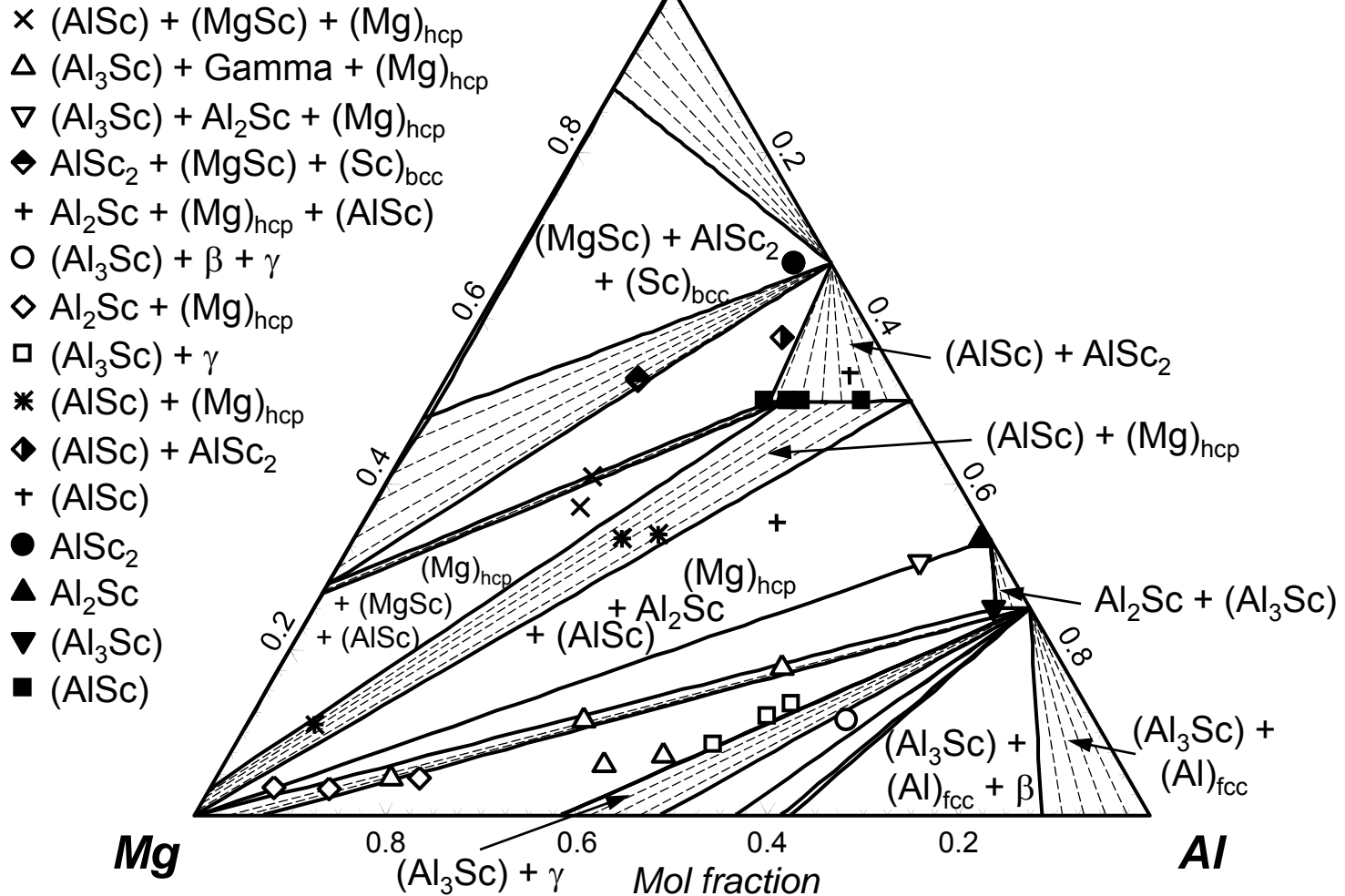


Figure 15: Calculated isothermal section of the Mg-Al-Sc system at 350°C compared with experimental data [22].

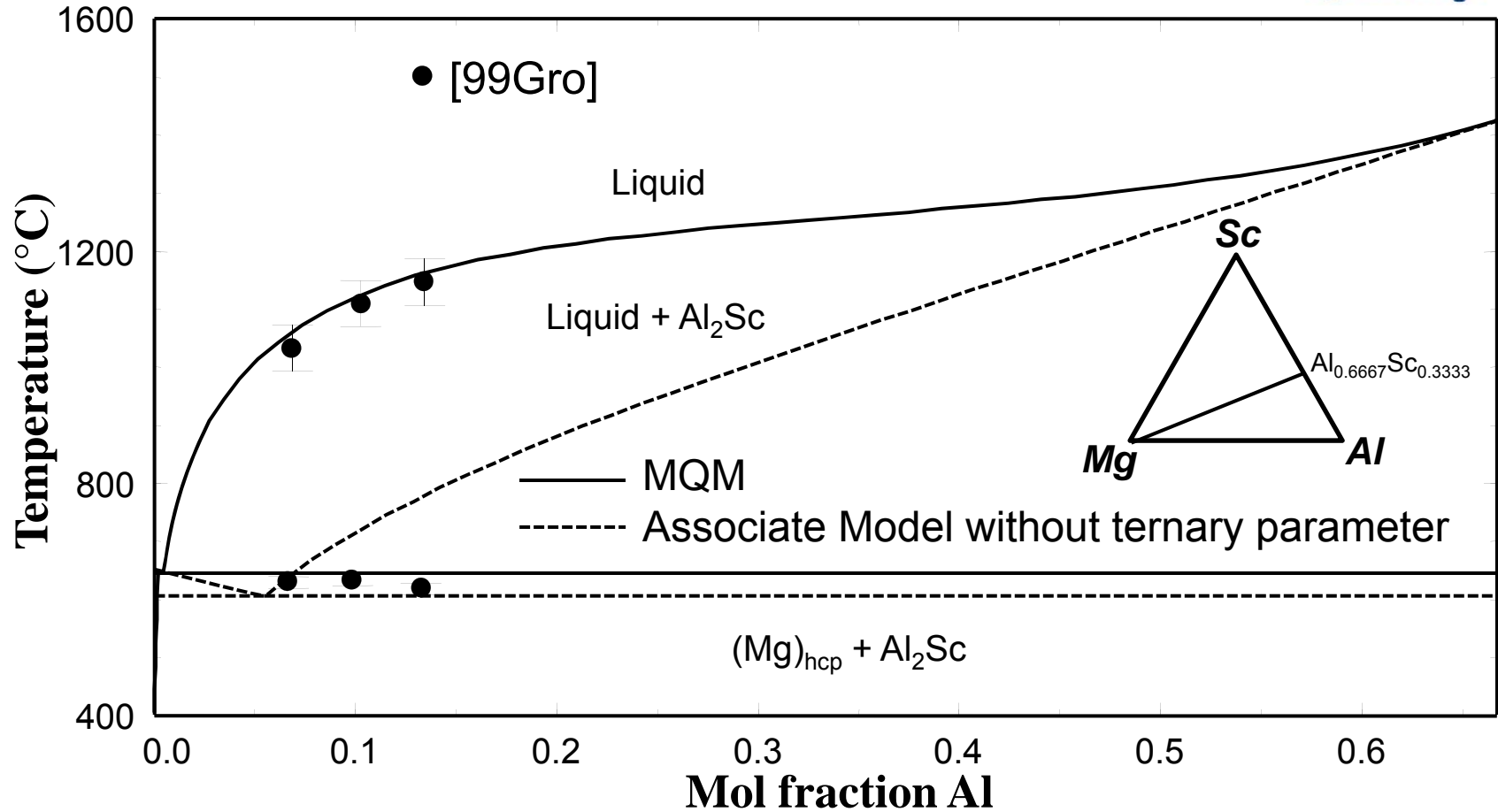


Figure 16: Calculated section of the Mg-Al-Sc system along the Al_{0.6667}Sc_{0.3333}-Mg (Al₂Sc-Mg) join using the MQM (with no ternary parameters), or the associate model without ternary parameters, compared to experimental data [19, 50].

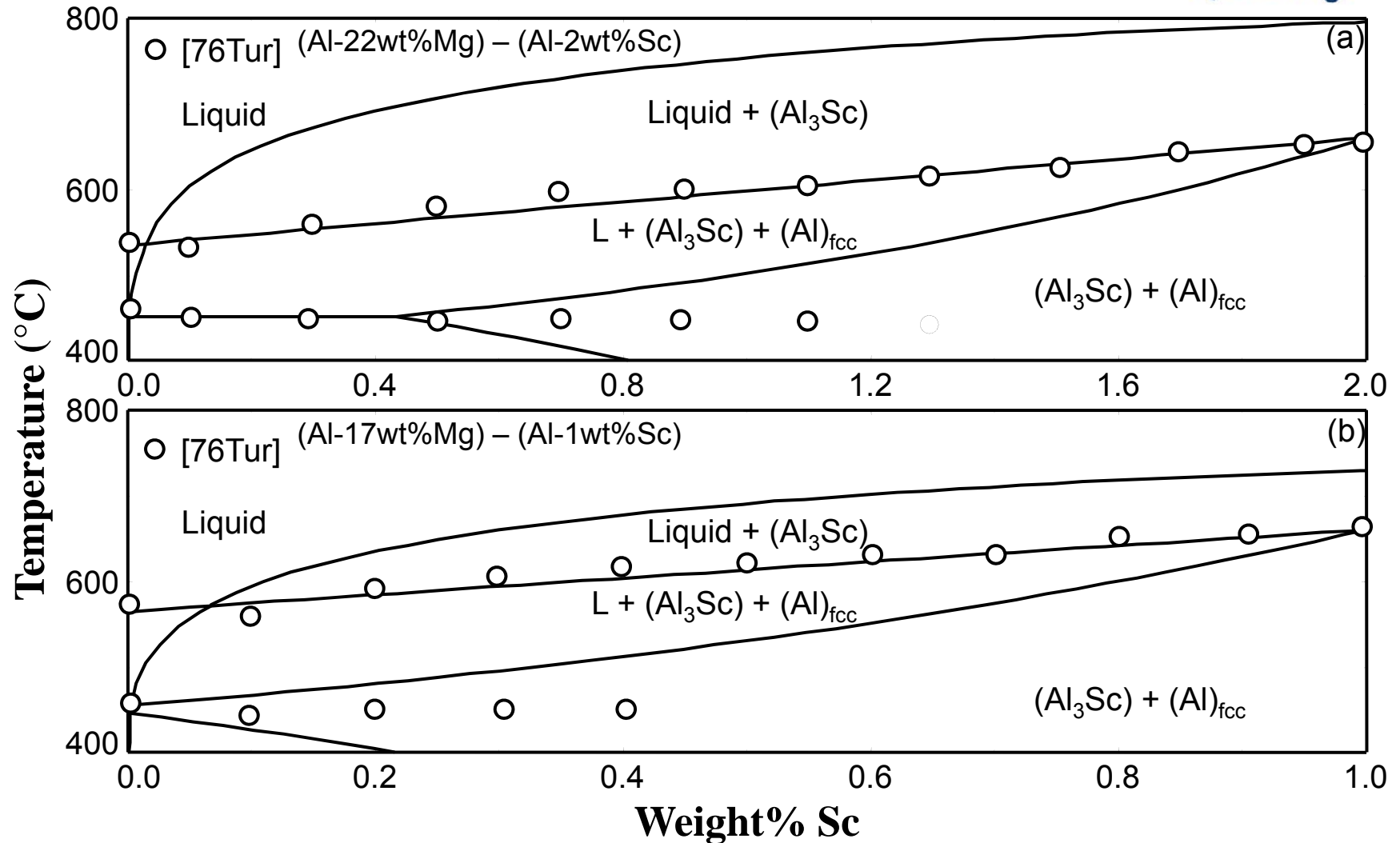


Figure 17: Calculated sections of the Mg-Al-Sc system along the (a) (Al-22wt%Mg) -(Al-2wt%Sc), (b) (Al-17wt%Mg)-(Al-1wt%Sc) joins compared with experimental data [53].

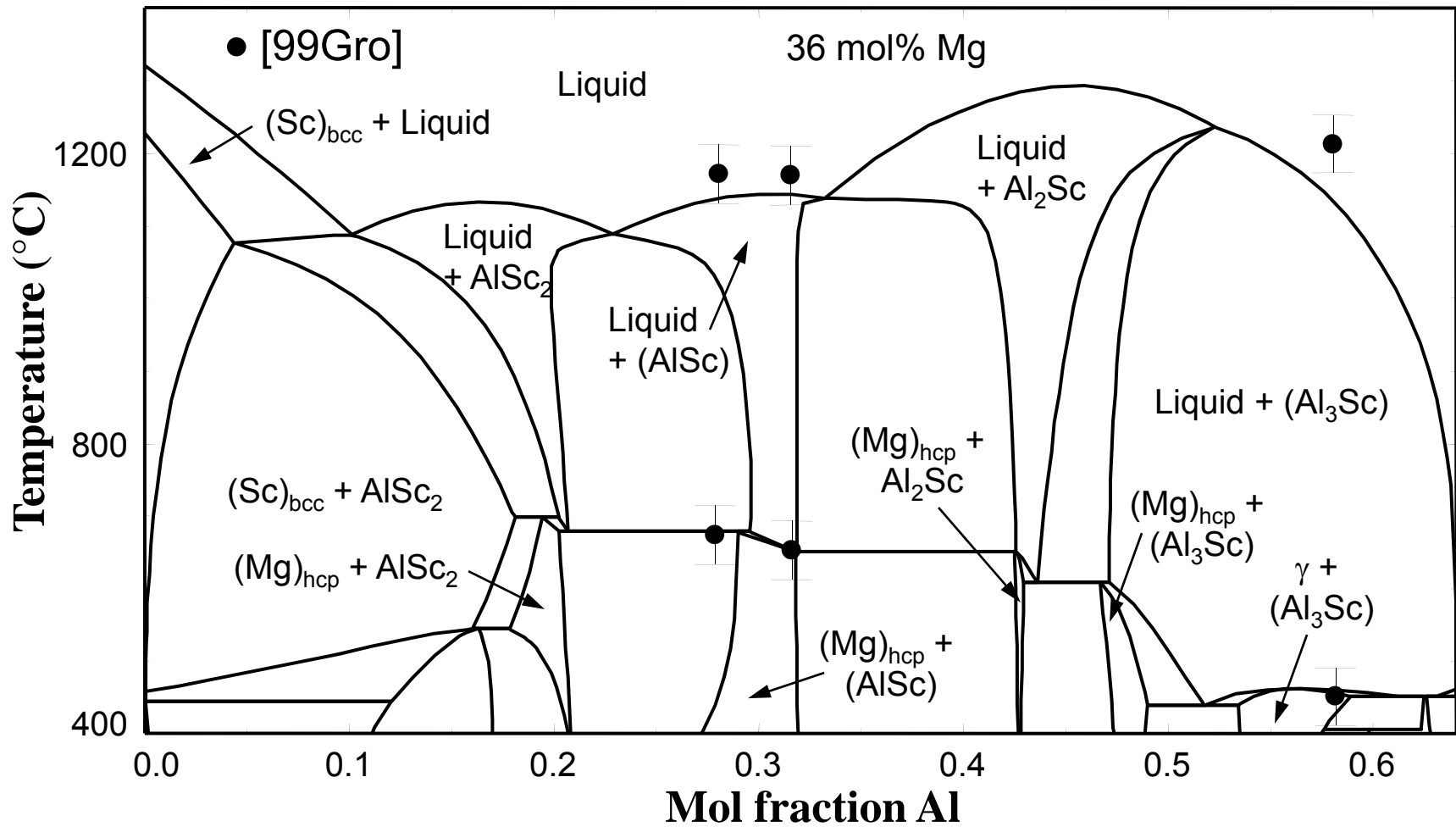


Figure 18: Calculated section of the Mg-Al-Sc system at $X_{\text{Mg}} = 0.36$ compared with experimental data [22].

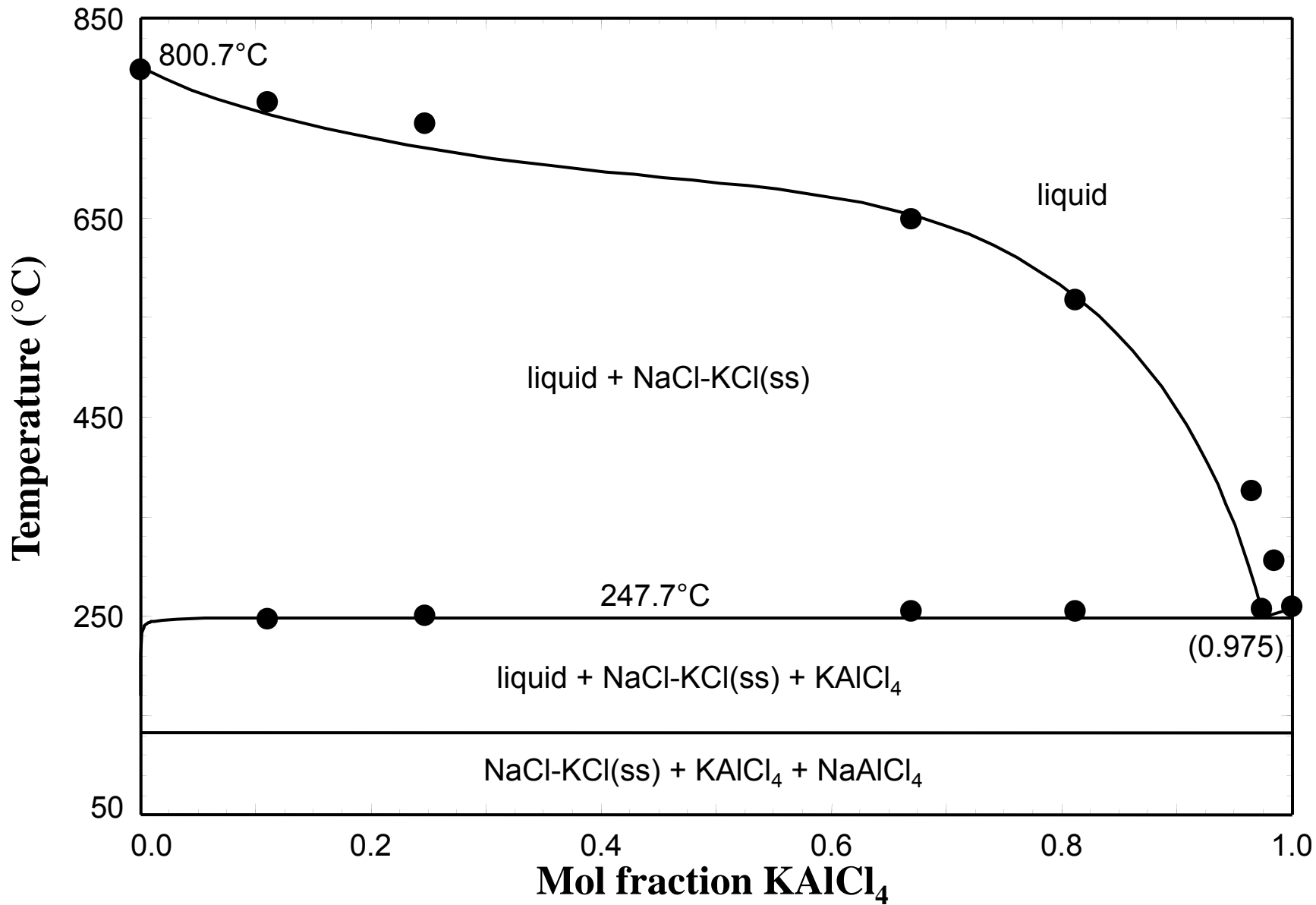


Figure 20: Calculated (NaCl + KAlCl₄) quasibinary phase diagram compared with experimental data [55].